HHS Public Access

Author manuscript

Neuron. Author manuscript; available in PMC 2022 September 01.

Published in final edited form as:

Neuron. 2021 September 01; 109(17): 2691–2706.e5. doi:10.1016/j.neuron.2021.06.015.

IL-23/IL-17A/TRPV1 Axis Produces Mechanical Pain via Macrophage-Sensory Neuron Crosstalk in Female Mice

Xin Luo[1], **Ouyang Chen**[1,2], **Zilong Wang**[1], **Sangsu Bang**[1], **Jasmine Ji**[1], **Sang Hoon Lee**[3], **Yul Huh**[1,2], **Kenta Furutani**[1], **Qianru He**[1], **Xueshu Tao**[1], **Mei-Chuan Ko**[4], **Andrey Bortsov**[1], **Christopher R Donnelly**[1], **Yong Chen**[5], **Andrea Nackley**[1,6], **Temugin Berta**[3], **Ru-Rong Ji**[1,2,7,8]

[1]Center for Translational Pain Medicine, Department of Anesthesiology, Duke University Medical Center, Durham, North Carolina, USA

[2]Department of Cell Biology, Duke University Medical Center, Durham, North Carolina, USA

[3]Pain Research Center, Department of Anesthesiology, University of Cincinnati College of Medicine, Cincinnati, Ohio, USA

[4]Department of Physiology and Pharmacology, Wake Forest School of Medicine, Winston-Salem, NC, USA

[5]Department of Neurology, Duke University Medical Center, Durham, North Carolina, USA

[6]Department of Pharmacology and Cancer Biology, Duke University Medical Center, Durham, North Carolina, USA

[7]Department of Neurobiology, Duke University Medical Center, Durham, North Carolina, USA

[8]Lead author: ru-rong.ji@duke.edu

SUMMARY

Although sex dimorphism is increasingly recognized as an important factor in pain, female-specific pain signaling is not well-studied. Here we report that administration of IL-23 produces mechanical pain (mechanical allodynia) in female, but not male mice, and chemotherapy-induced mechanical pain is selectively impaired in female mice lacking *Il23* or *Il23r*. IL-23-induced pain is promoted by estrogen but suppressed by androgen, suggesting an involvement of sex hormones. IL-23 requires C-fiber nociceptors and TRPV1 to produce pain but does not directly activate nociceptor neurons. Notably, IL-23 requires IL-17A release from macrophages to evoke mechanical pain in females. Low dose IL-17A directly activates nociceptors and

Correspondence should be addressed to: Ru-Rong Ji (Tel: 919-684-9387), Center for Translational Pain Medicine, Department of Anesthesiology, Duke University Medical Center, Durham, North Carolina, NC 27710, USA, ru-rong.ji@duke.edu, Xin Luo: xin.luo21@hotmail.com.

AUTHOR CONTRIBUTIONS

X.L. and R.R.J developed the project. X.L, O.C., Z.W., S.B., J.J., K.F., Q.H., X.T., A.B. conducted experiments and analyzed data; S.L. conducted qPCR experiment under supervision of T.B. M.C.K provided monkey DRG tissue. T.B., C.R.D., A.N., Y.C. participated in project discussion. X.L. and R.R.J. wrote the manuscript; Y.H., C.R.D., A.B., T.B., A.N., Y.C. and M.C.K and other co-authors edited the manuscript.

induces mechanical pain only in females. Finally, deletion of estrogen receptor subunit α (ERα) in TRPV1$^+$ nociceptors abolishes IL-23- and IL-17-induced pain in females. These findings demonstrate that the IL-23/IL-17A/TRPV1 axis regulates female-specific mechanical pain via neuro-immune interactions. Our study also reveals sex dimorphism at both immune and neuronal levels.

eTOC blurb

In this issue of *Neuron*, Luo et al., describe how IL-23, produced by macrophages, regulates mechanical pain in female mice, via IL-17 release, and subsequent activation of IL-17 receptor and TRPV1 in nociceptors, and therefore, offer a mechanistic insight into sex dimorphism in female pain through immune and neuronal regulations.

Keywords

Dorsal root ganglion; estrogen receptor α; IL-17; IL-23; macrophage; mechanical allodynia; nociceptor

INTRODUCTION

Sex dimorphism in chronic pain is a well-recognized clinical phenomenon, as females are more likely to suffer from chronic pain conditions, such as neuropathic pain, chronic fatigue syndrome, and fibromyalgia (Fillingim et al., 2009; Maixner and Humphrey, 1993). Emerging studies suggest sex differences in neuroimmune modulation of pain (Mogil, 2020). For example, spinal microglia regulate neuropathic pain selectively in male mice (Sorge et al., 2015), and microglia exhibit male-specific regulation of pain through Toll-like receptor 4, P2X4 receptor, and p38 MAP kinase (Chen et al., 2018b; Mapplebeck et al., 2018; Sorge et al., 2011; Taves et al., 2016). Macrophages are increasingly appreciated to play important roles in the pathogenesis and resolution of pain (Bang et al., 2018; Chen et al., 2020a). Macrophage activation in dorsal root ganglion (DRG) promotes pain in both sexes (Lopes et al., 2017; Luo et al., 2019c; Yu et al., 2020). However, emerging evidence suggests that male and female macrophages may use distinct pathways to modulate pain. In a mouse model of chemotherapy-induced peripheral neuropathy (CIPN), macrophage Toll-like receptor 9 (TLR9) signaling drives mechanical pain only in male mice (Luo et al., 2019c). Yu et al. showed that neuronal colony-stimulating factor-1 (CSF-1) regulates macrophage expansion in DRGs in male mice in the spared nerve injury model (Yu et al., 2020). However, the mechanism by which macrophages contribute to pain pathogenesis in females remains unknown.

It is generally believed that macrophages induce pain through interactions with peripheral nociceptor neurons (Chen et al., 2020a). Nociceptors represent a heterogeneous population of unmyelinated C-fibers and myelinated A-δ fibers (Woolf and Ma, 2007). Transient receptor potential vanilloid type 1 (TRPV1) channels are mainly expressed on C-fiber nociceptors and integrate thermal, chemical, and other noxious stimuli into pain signals (Basbaum et al., 2009; Caterina and Julius, 2001). Macrophage-produced pro-inflammatory cytokines/chemokines such as TNF-α and CCL-2 act directly on nociceptors to elicit

nociceptor sensitization (peripheral sensitization) and trigger pain hypersensitivity via TRPV1 activation (Chen et al., 2020a). Notably, prolactin produces female-specific pain signaling via prolactin receptor expressed by nociceptors (Chen et al., 2020b; Patil et al., 2019). Prolactin modulates TRPV1 activity in female sensory neurons in an estrogen-dependent manner (Diogenes et al., 2006). A recent study also demonstrated sex differences in nociceptor translational regulations (translatomes) (Tavares-Ferreira et al., 2020).

Interleukin 23 (IL-23) is a pro-inflammatory cytokine member of the interleukin 12 (IL-12) family and is released by antigen-presenting cells such as dendritic cells and macrophages (Gaffen et al., 2014). IL-23 exerts its functions through IL-23 receptor (IL-23R) in immune cells (e.g., T helper 17 cells) and drives the release of interleukin 17A (IL-17A) (Gaffen et al., 2014). Of note, the IL-23/IL-17 axis is essential for the pathogenesis of multiple inflammatory diseases, such as psoriasis and inflammatory bowel disease (van der Fits et al., 2009). Recently, IL-23 was found to induce a unique phenotype of macrophages (M-IL-23) that is distinct from conventional proinflammatory M1 and anti-inflammatory M2 phenotypes by unique production of IL-17A (Hou et al., 2018). IL-17A is a pro-inflammatory cytokine member in the IL-17 family and mediates pain through IL-17 receptor A (IL-17RA) that is known to be expressed by nociceptors (Luo et al., 2019a; Richter et al., 2012). In the present study, we investigated how peripheral IL-23 signaling modulates pain in male and female mice. Our findings demonstrate that IL-23 is necessary and sufficient to produce mechanical pain only in female mice. Furthermore, IL-23 signaling drives macrophage release of IL-17A, which enhances nociceptor excitability via IL-17RA to promote mechanical pain in females. These findings provide new insights into multi-level sex dimorphism arising from macrophage-neuron crosstalk in persistent pain states.

RESULTS

IL-23 drives female-specific mechanical allodynia in naive mice

We first measured the behavioral effects of intraplantar (I.PL.) injections of IL-23 at various doses (1, 10 and 100 ng) in naïve male and female mice. Von Frey testing showed that I.PL. IL-23 produced mechanical allodynia in females in a dose-dependent manner, as indicated by decreased paw withdrawal threshold (PWT) compared to PBS vehicle (Figure 1A): 1 ng IL-23 did not alter PWT to produce mechanical pain; 10 ng IL-23 induced transient mechanical pain at 0.5h; but 100 ng IL-23 evoked persistent mechanical pain for > 5h (Figure 1A). In contrast, these doses (1–100 ng) of IL-23 failed to produce mechanical pain in male mice (Figure 1A). The area under curve (AUC) analysis also revealed striking sex differences in IL-23-elicited mechanical pain (Figure S1A). Hargreaves and acetone tests showed that I.PL. IL-23 (1–100 ng) failed to evoke thermal or cold hypersensitivity in either sex, (Figures 1B–1C). IL-23 receptor (IL-23R) is the only known receptor of IL-23 (Gaffen et al., 2014). Notably, IL-23-evoked mechanical allodynia was abolished in *Il23r*$^{-/-}$ female mice (Figure 1D), suggesting a specific effect of IL-23 that is mediated by IL-23R. Furthermore, IL-23-induced mechanical pain in female mice was reversed by I.PL. injection of IL-23R antagonist P2305 (Quiniou et al., 2014) (Figure 1E). In contrast, IL-12, a family member of IL-23, evoked mechanical allodynia in both sexes, suggesting a distinct action of IL-23 in mediating female-specific mechanical pain (Figure S1B).

We further investigated whether IL-23 administration produced signatures of ongoing pain using a two-chamber conditioned place aversion (CPA) assay. Following pre-conditioning, mice were pretreated with I.PL. IL-23 (100 ng) or vehicle 1 h before testing, followed by repeated stimulation with a sub-threshold von Frey fiber (0.04 g) applied to the ipsilateral hindpaw of both male and female mice. While this stimulus is normally innocuous to naïve mice, von Frey fiber stimulation produced marked aversion in IL-23-treated female mice compared to the vehicle group. The same stimulation failed to produce aversion in male counterparts (Figures 1F–1H).

We also tested the intrathecal (I.T.) injection of IL-23, as this injection route can target cells in the spinal cord and DRGs (Donnelly et al., 2021). The result showed that I.T. injection of 100 ng of IL-23 also produced female-specific mechanical pain (Figure 1I). Taken together, our results suggest that IL-23 signaling drives mechanical pain through IL-23R in female mice.

IL-23 and IL-23R regulate chemotherapy-induced mechanical pain in females

To investigate the role of IL-23 signaling in chronic pain, we used a mouse model of CIPN in both sexes, produced by injection with the chemotherapeutic agent paclitaxel (PTX). This CIPN model allowed us to collect DRGs at all the spine levels for various analyses including flow cytometry analysis (Liu et al., 2014). We employed different approaches to determine the contribution of IL-23/IL-23R axis to CIPN. First, we collected serum and DRGs from naïve mice and PTX-treated mice on day 7, when neuropathic pain is fully developed in association with marked immune cell infiltration in DRGs (Luo et al., 2019c). ELISA data revealed a significant increase of IL-23 in serum and DRGs of female CIPN mice as compared to female naïve mice (Figures 2A–2B). By contrast, we did not observe IL-23 increases in serum and DRGs of male mice following CIPN (Figures 2A–2B). These data suggest that CIPN results in both systemic and local upregulations of IL-23 in females. Second, we examined PTX-induced mechanical pain in wildtype (WT) mice and knockout (KO) mice lacking either the ligand (*Il23*$^{-/-}$) or receptor (*Il23r*$^{-/-}$) of the IL-23/IL-23R axis. Notably, the baseline mechanical pain was unaltered in *Il23*$^{-/-}$and *Il23r*$^{-/-}$ mice of either sex, compared to corresponding WT controls (Figures 2C–2D). PTX produced mechanical pain in WT mice of both sexes, but *Il23* or *Il23r* deficiency reduced PTX-induced mechanical pain in female but not male mice (Figures 2C–2D). Of interest *Il23* or *Il23r* deficiency reduced mechanical pain in the early-phase (day 3) and late-phase (2–3w) of PTX-treated females, without changing mechanical pain in the mid-phase (7d and 10d) (Figures 2C–2D). PTX also evoked cold pain (cold allodynia) in both sexes, which was not affected by *Il23* or *Il23r* deficiency (Figures S2A–S2B). Third, we assessed the sex effects of IL-23R antagonist P2305 in different pain models. Mechanical pain after CIPN was reversed by I.PL. or I.T. administration of the IL-23R antagonist P2305 in female but not male mice (Figures 2E–2F). Additionally, I.PL. injection of P2305 reduced neuropathic pain (mechanical allodynia) in females after nerve injury (chronic constriction injury, CCI) and diabetic neuropathy, induced by streptozotoxin (STZ) (Figures 2G–2H). We also tested formalin-induced acute inflammatory pain in both sexes and found that I.PL. P2305 reduced Phase II spontaneous pain in the formalin model in female mice (Figures 2I–2J). Collectively, these results suggest that IL-23/IL-23R axis is required for

generating female-specific mechanical allodynia (neuropathic pain) and spontaneous pain (inflammatory pain).

Sex hormones differentially regulate IL-23-mediated mechanical pain

To further understand the mechanisms underlying sex dimorphism of IL-23 signaling in pain, we used multiple surgical and pharmacological approaches to investigate the impact of estrogen signaling in this process. Estrogen deficiency by ovariectomy (OVX) largely prevented IL-23-induced pain in female OVX mice vs. sham control mice (Figure 3A). Concordantly, systemic pretreatment of estrogen (2 mg/kg, subcutaneously) enabled IL-23-induced pain in males (Figure 3B). This effect was mediated by estrogen receptor α (ERα) but not estrogen receptor β (ERβ), because subcutaneous treatment of ERα agonist PPT but not ERβ agonist AC186 (2 mg/kg) could enable IL-23-induced pain in males (Figure 3B). Estrogen deficiency also relieved PTX-induced mechanical pain at 3 d and 2 w in females (Figure S3A), as mechanical allodynia at these time points was dependent on IL-23/IL23R signaling (Figures 2C–2D). Consistently, we found that co-intraplantar injection of the ERα antagonist MPP (30 μg) with IL-23 prevented IL-23-induced mechanical pain in female mice (Figure 3C).

We then asked why male mice are insensitive to IL-23. We observed that androgen deficiency by orchiectomy (ORX) enabled IL-23-produced mechanical pain in ORX males vs. sham-operated mice (Figure 3D). Furthermore, testosterone treatment (2 mg/kg, subcutaneous) inhibited IL-23-induced pain in female mice (Figure 3E). Co-intraplantar injection of the androgen receptor (AR) antagonist Ailanthone (30 μg) with IL-23 enabled IL-23-induced mechanical pain in male mice (Figure 3F). In the CIPN model, androgen deficiency did not alter mechanical pain (Figure S3B). IP.L. IL-23R antagonist P2305 (10 μg), however, did reduce paclitaxel-induced mechanical pain in male ORX mice but not female OVX mice (Figure 3G). Additionally, I.PL. injection of the ERα antagonist MMP (30 μg) decreased PTX-induced mechanical allodynia in females but not males (Figure S3C), showing no effects on cold allodynia (Figure S3D). Together, these findings suggest crucial roles of 1) estrogen in promoting IL-23-mediated mechanical pain via ERα and 2) androgen (testosterone) in suppressing this pain.

IL-23-induced mechanical pain requires macrophages and C-fiber nociceptors

We further assessed the cellular mechanisms underlying IL-23-induced pain. Ablation of macrophages/monocytes by intravenous injection of macrophages/monocytes toxin, clodronate liposomes (Bang et al., 2018), completely prevented IL-23-evoked mechanical pain (Figure 4A). As macrophages are an important biological source of IL-23 (Gaffen et al., 2014; Hou et al., 2018), we measured IL-23 release in peritoneal macrophage cultures by ELISA assay. We found that female macrophages displayed higher levels of IL-23 release in culture medium following PTX incubation (1 μg/ml, 16h) compared to male macrophages (Figure 4B). Chemotherapy-activated macrophages are sufficient to evoke mechanical pain by adoptive transfer of macrophages (Luo et al., 2019c). Figure 4C shows mechanical pain following I.PL. injection of PTX-activated macrophages in both sex-matched manner (male to male and female to female) and cross-matched manner (male to female and female to male). We observed that female macrophages produced more

potent and persistent mechanical pain in female vs. male recipients, whereas male recipients displayed greater mechanical pain from male donors than female donors (Figure 4C), in support of a sex-based macrophage-mediated pain. Flow cytometry analysis revealed that female DRGs displayed larger IL-23$^+$ subset of macrophages than male DRGs under both naïve and CIPN conditions (Figures S4A–4B, Table S1). Female DRGs also displayed larger subset of IL-23R$^+$ macrophages under both naïve and CIPN conditions (Figures S4C–4D). In peritoneal macrophage culture, PTX incubation (1 μg/ml, 16 h) significantly increased the population of IL-23$^+$ macrophages in both females and males (Figures S4E–4F). IL-23R$^+$ population of macrophages was significantly larger in female vs. male peritoneal macrophages after PTX treatment (Figures S4G–4H). We also performed transfer of PTX-activated macrophages from WT, *Il23*$^{-/-}$, and *Il23r*$^{-/-}$ mice. WT macrophages evoked sustained mechanical pain in both sexes for > 3 days (Figure 4D). However, *Il23*$^{-/-}$ macrophages failed to produce mechanical pain in female recipients at 2d and 3d time points (Figure 4D). There was no difference between WT and *Il23*$^{-/-}$ macrophage-induced mechanical pain in male recipients (Figure 4D). Consistently, *Il23r*$^{-/-}$ macrophages also produced less and more transient mechanical pain compared to WT macrophages only in females (Figure 4E). Given a critical role of T cells in mediating IL-23 signaling in disease conditions such as psoriasis (Riol-Blanco et al., 2014), we also tested IL-23-evoked pain in T cell deficient nude mice and *Rag1*$^{-/-}$ mice. Strikingly, I.PL. IL-23 was fully capable of inducing mechanical allodynia in both lines of immune-deficient mice (Figure 4F), arguing against an involvement of T cells. These results suggest that macrophages are both required and sufficient to mediate IL-23-produced mechanical pain in females.

C-fiber and A-fiber sensory neurons mediate mechanical pain via distinct mechanisms (Hill and Bautista, 2020). Ablation of TRPV1$^+$ C-fibers by resiniferatoxin (RTX, subcutaneous injection for 3 continuous days at escalating doses of 30, 50 and 100 μg/kg) completely abolished mechanical pain induced by IL-23 (Figure 4G). We also blocked C-fibers or A-fibers (Aβ fibers) using QX-314 (6 mM) together with C-fiber activator capsaicin (Binshtok et al., 2007) and Aβ-fiber activator flagellin (Xu et al., 2015). I.PL. pre-treatment with QX-314 plus 5 μg capsaicin, but not QX314 plus 0.3 μg flagellin, prevented the IL-23 evoked mechanical pain in female mice when compared to control mice treated with QX314, suggesting the involvement of C-fibers but not Aβ fibers in this process (Figure 4H). However, ablation of non-peptidergic nociceptors (IB4-binding) with IB4-saporin had no effect on IL-23-evoked mechanical pain (Figure 4I).

Our results indicated that IL-23-induced pain requires TRPV1$^+$ C-fiber nociceptors and led us to investigate whether IL-23 would directly modulate nociceptor activities to evoke pain. We used Ca^{2+} imaging to measure acute effect of IL-23 on dissociated DRG sensory neurons from male and female *Advillin*^{Cre}*/GCamp6f* mice (Wang et al., 2020a). Our results showed that IL-23, even at a high concentration (100 ng/ml, 2 min), had no effect on Ca^{2+} signaling in sensory neurons from either females or males. As positive control, capsaicin (300 ng/ml, 2 min) caused robust Ca^{2+} influx in ~20% DRG neurons without sex difference (Figures 4J–4K). IL-23 may excite nociceptors via mechanisms other than Ca^{2+} signaling. To address this question, we used electrophysiology to test the effects of IL-23 in dissociated small-sized mouse DRG neurons from females. Whole-cell patch-clamp recording revealed that IL-23 bath application (100 ng/ml) did not alter the number of action potential (AP)

discharges in response to suprathreshold current injection (Figures 4L–4M). Taken together, our evidence indicates that DRG sensory neurons are not directly activated by IL-23.

IL-17A is the downstream effector of macrophage IL-23 signaling in pain

IL-17A expression is a downstream effector of IL-23 signaling in T cells (Gaffen et al., 2014) and macrophages (Hou et al., 2018). We observed that PTX (1 μg/ml, 16h) increased IL-17A levels in both male and female macrophages. Notably, *Il23r*$^{-/-}$ suppressed IL-17A production only in female PTX-treated macrophages as compared to male counterparts (Figures 5A). Importantly, IL-23 incubation (100 ng/ml, 16h) was sufficient to induce IL-17A secretion in female but not male peritoneal macrophage cultures (Figure 5B).

Previous studies have shown pro-nociceptive effects of I.PL. IL-17A in rodents (Kim and Moalem-Taylor, 2011; Meng et al., 2013). However, only male animals were tested in these studies. We found IL-17A evoked mechanical pain in female mice in a dose (1–100 ng) and time (0.5–3h) dependent manner (Figure 5C). In contrast, only IL-17A at 100 ng produced a transient mechanical pain (1h) in males (Figure 5C). The area under curve (AUC) analysis also revealed striking sex differences in IP.L. IL-17A-elicited mechanical pain (Figure 5F). Like IL-23, IL-17A (1–100 ng) failed to produce thermal or cold hypersensitivity in mice of either sex (Figures 5D–5E). Co-intraplantar injection of IL-17A or IL-17RA neutralizing antibodies (2 μg) with IL-23 (100 ng) blocked the IL-23-induced mechanical pain in females (Figure 5G). Interestingly, ablation of macrophages by intravenous injection of clodronate had no effect on IL-17A-induced mechanical pain in females (Figure 5H). IL-17A-induced mechanical pain was not altered in *Il23*$^{-/-}$ mice (Figure 5I). Additionally, estrogen deficiency after OVX prevented IL-17A-induced pain in females, whereas ORX enabled low dose IL-17A-induced pain in males (Figures 5J and 5K). There results suggest 1) IL-17 is a downstream event of IL-23 signaling in mechanical pain and 2) IL-17 -induced mechanical pain also depends on sex hormones.

Next, we investigated the contribution of IL-17A to mechanical pain after CIPN in both sexes. PTX enhanced serum IL-17A in both sexes with a slightly higher level in females (Figure 5L). However, PTX increased DRG levels of IL-17A only in female mice (Figure 5M). Flow cytometry revealed that female DRGs exhibited a larger population of IL-17A^{+} and IL-23R^{+}IL-17A^{+} macrophages than male DRGs under CIPN (Figures S5A–5D, Table S1). In peritoneal macrophage cultures, PTX increased ratios of IL-17A^{+} subset and IL-23R^{+}IL-17A^{+} subset in female macrophages but not male counterparts (Figures S5E–5H). Collectively, these data suggest (1) IL-17A production and release in macrophages requires IL-23/IL-23R axis in females and (2) IL-17A is the downstream effector of macrophage IL-23 signaling in female mechanical pain.

Low dose of IL-17A activates mouse and NHP DRG nociceptor neurons

Previous electrophysiological studies in male animals showed that IL-17A (50 and 100 ng/ml) increased nociceptor excitability in DRG neurons (Richter et al., 2012). We performed Ca^{2+} imaging to examine nociceptor activation by IL-17A in DRG sensory neurons dissociated from male and female *Advillin*^{Cre}*/GCamp6f* mice (Wang et al., 2020a). Acute incubation of IL-17A (10 ng/ml, 2 min) evoked Ca^{2+} influx in 5.7% of sensory

neurons in females but none in males (Figures 6A–6C). High concentration of IL-17A (100 ng/ml) evoked Ca^{2+} increase in 11.9% female DRG neurons but only 6.1% male sensory neurons (Figures S6A–S6C). These findings suggest a sex-dependent activation of nociceptors by IL-17A. We also applied whole-cell patch clamp recording to test the effects of a very low concentration of IL-17A (1 ng/ml, 2 min) on the excitability of dissociated small-sized DRG neurons (<25 μm in diameter, presumed nociceptors, 16–40h in culture) from male and female mice. Strikingly 1 ng/ml of IL-17A only increased action potential firing in female DRG neurons (Figures 6D–6E) not in male DRG neurons (Figures 6F–6G). Thus, IL-17A activates mouse sensory neurons in a sex-dependent manner.

To enhance the translational potential of these findings, we also investigated the action of IL-17A in nonhuman primate (NHP) DRG neurons from 3 rhesus macaques (*Macaca muletta*; one male and two female). Low dose of monkey IL-17A (1 ng/ml) increased action potential firing in small-sized DRG neurons (<50 μm in diameter) from the female rhesus macaque (Figures 6G–6H), but failed to do so in DRG neurons of the male rhesus macaque (Figures 6H–6K).

Furthermore, we tested IL-17A actions in human DRG neuron cultures we prepared from disease-free donors (Chang et al., 2018). At a dose of 10 ng/ml, human IL-17A increased action potential discharges in small-sized human DRG neurons (<55 μm in diameter) from both male and female donors (Figures S6D–S6F). Human IL-17A (10 ng/ml) also altered resting membrane potential but not rheobase in these neurons (Figures S6G–S6H). Strikingly, at the dose of 1 ng/ml, IL-17A also increased nociceptor excitability in a female donor (Figures S6I–S6J).

TRPV1 is required for mediating IL-23 and IL-17A produced mechanical pain in females

TRPV1 and TRPA1 are critical Ca^{2+} channels for generating pain (Caterina and Julius, 2001; Patapoutian et al., 2009). We asked whether these channels are required for IL-23-induced nociception using genetic and pharmacological approaches (Figures 7A–7D). Notably, *Trpv1* deletion abolished mechanical pain induced by I.PL. and I.T. injection of 100 ng IL-23 in females (Figures 7A), and I.PL. IL-23R antagonist (P2305, 10 μg) failed to reduce PTX-induced mechanical pain in $Trpv1^{-/-}$ mice in both sexes (Figure 7B). By contrast, I.PL or I.T. injection of IL-23 effectively evoked mechanical pain in $Trpa1^{-/-}$ female mice (Figure 7C), and furthermore, P2305 reduced PTX-evoked mechanical pain only in $Trpa1^{-/-}$ female mice (Figure 7D). These findings suggest that TRPV1 but not TRPA1 is indispensable for IL-23-induced mechanical pain in females.

Capsaicin produces spontaneous pain, thermal hyperalgesia, as well as primary and secondary mechanical hyperalgesia/allodynia in rodents and humans (Caterina and Julius, 2001; Simone et al., 1989) (Figures S7A and S7B). I.PL. capsaicin evoked dose-dependent mechanical pain in males and females, but female mice exhibited greater and more persistent mechanical pain (Figure 7E and Figure S7B). Interestingly, very low dose of capsaicin (50 ng) produced mechanical allodynia only in females (Figure 7E). We did not see significant sex differences in capsaicin-evoked spontaneous pain, although there was a trend of greater pain in females (Figure S7A). Capsaicin-induced mechanical pain in females was abolished after C-fiber ablation by RTX (Figure S7C) and also abrogated in OVX mice

with estrogen deficiency (Figure 7F). Conversely, ORX with androgen deficiency enabled low-dose capsaicin to induce mechanical pain in males (Figure 7G).

We next examined whether IL-17A requires C-fibers and TRPV1 to produce mechanical pain in females. *In situ* hybridization using RNAscope revealed that ~40% mouse DRG neurons expressed *Trpv1* or *Il17r* mRNA, with comparable expression in both sexes (Figures 7I–7J). *Trpv1* mRNA and *Il17r* mRNA were highly co-localized in nociceptors, and ~70% *Il17r*$^{+}$ neurons express *Trpv1* mRNA in both sexes (Figure 7K). Notably, mechanical allodynia at 0.5h by I.PL. IL-17A in female mice was transiently reduced after C-fiber ablation and *Trpv1* deficiency (Figures 7L and 7M). Compared to female mice, male mice exhibited less mechanical pain following I.PL. IL-17A (Figure 5C) and this mechanical pain in male mice was not affected after C-fiber ablation and *Trpv1* deficiency (Figures S7D–S7E), suggesting that IL-17A signaling links to TRPV1 only in female nociceptors. Ca^{2+} imaging indicated that 4.67% and 10.59% sensory neurons responded to 10 and 100 ng/ml of IL-17A, respectively, and these neurons also responded to 300 nM capsaicin in female neurons, implicating that IL-17A sensitized TRPV1 in a dose-dependent manner (Figure 7N–7O). Of note, TRPV1 antagonist AMG9810 (3 μM) blocked the IL-17A-evoked Ca^{2+} response in female DRG neurons (Figures S7F–S7G). *Trpv1* deletion also abolished the IL-17A potentiation of action potential firing in female DRG neurons (Figure 7P). Collectively, these data indicate that TRPV1 is crucial for IL-17A-induced nociceptor activation and mechanical pain in females.

ERα receptor in C-fiber nociceptors regulates IL-23 and IL-17 induced pain in females

RNA-seq analyses demonstrated that mouse DRG neurons express both ERα and ERβ subunits of estrogen receptors (Tavares-Ferreira et al., 2020; Zheng et al., 2019). Because IL-23-induced mechanical pain required ERα but not ERβ (Figure 3B), we investigated how ERα in nociceptors regulates mechanical pain in females. *In situ* hybridization revealed *Erα* expression in >40% of mouse DRG neurons in both sexes (Figures 8A–8B). In particular, we observed co-localization of *Il17ra*, *Tprv1*, and *Erα* mRNAs in 10.45% female DRG neurons and 10.28% male DRG neurons (Figure 8C). These nociceptors had average diameters of ≤ 20 μm in both sexes (Figure 8D). Thus, TRPV1^{+} nociceptors co-express IL-17R and ERα providing a cellular base for interactions among these receptors.

To determine the role of ERα in TRPV1^{+} nociceptors for mechanical pain, we generated *Erα* conditional knockout mice (cKO) by crossing *Erα*-floxed mice with *Trpv1*-Cre mice. Compared to *Trpv1*-Cre female mice, cKO female mice displayed a partial reduction in capsaicin-induced spontaneous pain (Figure 8E) but a complete blockade of I.PL. IL-23-elicted mechanical allodynia (Figure 8F). Furthermore, this conditional deletion abolished I.PL. IL-17A- and capsaicin-induced mechanical pain in females (Figures 8G–8H). In male cKO mice, capsaicin-induced spontaneous pain was unaltered (Figure S8A). Estrogen enabled IL-23 (100 ng) and IL-17A (10 ng) to induce mechanical pain in *Trpv1*-Cre male mice, but these effects were lost in male cKO mice (Figures S8B and S8C). Additionally, ERα agonist PPT (1 ng/ml, 16h) enables IL-17A (10 ng/ml) to evoke Ca^{2+} influx in dissociated DRG sensory neurons from male *Advillin*^{Cre}*/GCamp6f* mice (Figures S8D and S8E).

Translatome analysis mice revealed no sex differences in *Trpv1*, *Il17ra*, *Erα*, and *Erβ* expression in Nav1.8^{+} nociceptors (Tavares-Ferreira et al., 2020), and the data were re-plotted in Figure S8F. We also conducted quantitative PCR analysis in human DRGs from both male and female donors (Figures 8I–8L). We found comparable expression of h*TRPV1* (Figure 8I), h*IL17R* (Figure 8J), and h*ERβ* (Figure 8L) in both sexes but higher *hERα* expression in female DRGs using two different sets of primers (Figure 8K, Figure S8G, Table S2). Finally, human plasma proteome profiles across the life span supported the translational relevance of this study: both serum IL-23 and IL-17A levels are higher in females (n=2146) compared to males (n=2117) (Lehallier et al., 2019), as plotted in Figures S8H and S8I.

DISCUSSION

Previous studies have demonstrated male-specific pain signaling in immune cells such as microglia (Chen et al., 2018b; Sorge et al., 2015) and macrophages (Luo et al., 2019c; Yu et al., 2020). Our present results demonstrate a previously unrecognized sex dimorphism at multiple cellular levels involving macrophages and nociceptors (Figure 8M). Notably, sex dimorphism in pain is not simply cell type dependent, and even within a given cell type (e.g., macrophages), there may be sex-selective signaling networks which differentially regulate pain. We previously demonstrated male-selective TLR9 signaling in macrophage regulation of pain (Luo et al., 2019c). Here we further demonstrated female-selective IL-23 signaling in macrophage regulation of pain. Using pharmacological, genetic, behavioral, and electrophysiological approaches, we showed that IL-23/IL-17/TRPV1 axis regulates mechanical pain in females. First, I.PL. IL-23 induced mechanical pain (mechanical allodynia) in female not male mice. Second, IL-23 does not activate nociceptors directly. Instead, IL-23 evokes mechanical pain in females indirectly via IL-17A release from macrophages. Third, low dose IL-17A activates nociceptors in mouse, monkey, and human DRG neurons isolated from females. Low dose IL-17A and capsaicin also induce mechanical pain in female mice. Fourth, both IL-23 and IL-17A require C-fiber nociceptors and TRPV1 to produce mechanical pain in females. Fifth, estrogen is essential for IL-23/IL-17A/TRPV1 axis to evoke mechanical pain in females and further enables IL-23 and IL-17A to produce mechanical pain in males via ER-α. Finally and importantly, ER-α expression by TRPV1^{+} nociceptors is necessary for inducing female mechanical pain by IL-23, IL-17A, and capsaicin. Previous studies have shown the involvement of IL-23 in chronic pain. Askari et al. reported a positive correlation between serum IL-23 levels and pain scores in osteoarthritis patients (Askari et al., 2016). I.T. injection of 2 μg of IL-23 produced long-lasting mechanical pain in male rats via a mechanism involving spinal astrocytes (Bian et al., 2014). We do not exclude the possibility that IL-23 at very high doses may produce pain in males. IL-23 also plays an active role in arthritic and inflammatory pain, using weight-bearing assay and sex-matched *Il23*$^{-/-}$ mice (Lee et al., 2020).

Our finding revealed an unconventional IL-23/IL-17 signaling axis in macrophage-macrophage and macrophage-nociceptor interactions in a sex-dependent manner. It is well established that IL-23/IL-17A axis regulates dendritic cell and T cell interaction, Th17 cell development, and IL-17A production (Gaffen et al., 2014; van der Fits et al., 2009). However, our results indicate that IL-23-induced pain does not depend on T cells. Instead,

our data suggested that chemotherapy may polarize resting macrophages into an IL-23^{+} subset in a female-dominant manner. Autocrine or paracrine IL-23 signaling was shown to amplify macrophage release of IL-17A in inflammatory bowel disease (Sun et al., 2020). IL-17A-producing macrophages also contribute to breast cancer (Zhu et al., 2008) and asthma (Song et al., 2008). Interestingly, IL-23 at a high concentration (100 ng/ml) failed to activate mouse DRG neurons, as revealed by both calcium imaging and electrophysiology results. Rather, our data support an indirect activation of nociceptors by the IL-23 cascade through IL-17A. Emerging evidence suggests that IL-17-mediated inflammation displays sex dimorphism. Scharff et al. demonstrated higher IL-17 levels in bladder tissue of females compared to males after urinary tract infections (Zychlinsky Scharff et al., 2019). House dust mites increased IL-17 levels in lung tissues of females moreso than males in a mouse model of asthma (Fuseini et al., 2018). Female mice also exhibit higher levels of IL-17A in nerve fibers and spinal cord compared to male mice after nerve injury (Noor et al., 2019). Our results suggest a female-dominant role of IL-17A in pain processing. At higher concentrations (50 and 100 ng/ml), IL-17A also increases nociceptor excitability in DRG neurons of male rats, and IL-17 sensitizes joint nociceptors to mechanical stimuli in arthritic pain (Richter et al., 2012). We found that low doses of IL-17A evoked mechanical pain, Ca^{2+} influx and action potentials in nociceptor neurons in a female-dominant manner. Given the rapid effects on nociceptors, IL-17RA may have a direct interaction with TRPV1 to facilitate TRPV1-mediated ion flux or cause rapid surface trafficking of TRPV1 through intracellular signaling (Zhang et al., 2005).

Our results also provide new insights into sex hormone regulation of pain. Using surgical and pharmacological means, we demonstrated that estrogen and androgen regulate IL-23-induced pain in females and males, respectively. Mechanistically, we revealed that nociceptor ERα is critical to regulate IL-23/IL-17A axis-mediated mechanical pain. Transcriptional profiles of C-fiber nociceptors indicated that neuronal expression of IL-17RA, TRPV1 and ERα was not sexually different in DRGs (Tavares-Ferreira et al., 2020). Using cKO mice that lack ERα in *Trpv1*$^{+}$ nociceptors, we found mechanical pain, induced by IL-23, IL-17A, or capsaicin was compromised in female cKO mice. It is unclear how estrogen/ERα signaling affects TRPV1^{+} C-fiber nociceptors. Estrogen (estradiol or E2) may not regulate *Tprv1* expression in sensory neurons (Diogenes et al., 2006), which is consistent with our result showing no sex difference in *Tprv1* expression in DRGs. Notably, a short incubation (10 min) of estrogen prevented TRPV1 desensitization in dissociated sensory neurons (Payrits et al., 2017). Estrogen also enhanced the TRPV1 agonist-induced mechanical hyperalgesia in OVX mice and ocular pain in OVX rats (Payrits et al., 2017; Yamagata et al., 2016). Furthermore, women exhibit higher pain intensity and unpleasantness than men following the topical administration of capsaicin (Frot et al., 2004). Capsaicin may induce mechanical pain via neurogenic inflammation and release of calcitonin gene-related peptide (CGRP) (Warwick et al., 2019). Notably, low dose of capsaicin (50 ng) produced mechanical pain in female mice (Figure 7E) and low dose of CGRP (1 pg) produces mechanical pain in female rats (Avona et al., 2019). Furthermore, mechanical allodynia is the most common pain modality to exhibit sex dimorphism in pain, induced by microglia and macrophages (Chen et al., 2018a; Luo et al., 2018; Luo et al., 2019b; Luo et al., 2019c; Sorge et al., 2015; Taves et al., 2016).

There remain some limitations of this study. Single-cell RNA sequencing data indicated that IL-17RA is widely expressed in various types of cells in mouse DRGs, including satellite glia and macrophages (Avraham et al., 2020). IL-17A signaling in these non-neuronal cells may contribute to pain processing along with sensory neurons, warranting further investigation. The sex dimorphism of capsaicin-evoked mechanical pain is promoted by estrogen in females and suppressed by androgen in males, implicating sex hormone homeostasis as a prerequisite for sex dimorphism in TRPV1-mediated mechanical pain. Further investigations will be needed to explore the intracellular mechanisms underlying how the IL-17RA$^+$/TRPV1$^+$/ERα$^+$ neuron subpopulation mediates mechanical pain in females. While this study focused on mechanical pain, future studies are warranted to investigate distinct mechanisms that regulate sex dimorphism in mechanical pain and thermal hyperalgesia. In addition to pro-nociceptive actions, peripheral and central macrophages may also regulate the resolution of pain through distinct signaling (Bang et al., 2018; Niehaus et al., 2021; Tonello et al., 2020), and it will be of great interest to investigate sex dependence in this unique pro-resolving function of macrophages.

In summary, our results demonstrate that IL-23/IL-17A/TRPV1 axis drives female-specific mechanical pain through macrophage-neuron crosstalk (Figure 8M), which would constitute a critical step forward in our understanding of sex dimorphism in chronic pain. At the immune cell level, female macrophages produce more IL-23 and IL-17A than male macrophages. At the sensory neuron level, female nociceptors are more sensitive to IL-17A challenge than male nociceptors. This multiple cellular signaling and macrophage-nociceptor interaction may amplify the sex-different pain signaling in a cascading manner. The translational relevance of this study is supported by our NHP and human data. IL-23/IL-17A axis is a key pathway in immune-related inflammatory diseases, and there are existing drugs to target this pathway (Gaffen et al., 2014). Our findings would encourage the field to re-examine the role of IL-23/IL-17A axis in chronic pain symptoms and develop precision pain-relief therapies for females.

STAR★METHODS

RESOURCE AVAILABILITY

Lead Contact—Further information and requests for resources and reagents should be directed to and will be fulfilled by the Lead Contact, Ru-Rong Ji (ru-rong.ji@duke.edu).

Materials Availability—Materials are available upon request. This study did not generate new unique reagents.

Data and Code Availability—Source data for all figures in the paper is available in Table S5.

No custom software was used in this study.

EXPERIMENTAL MODEL AND SUBJECT DETAILS

Animals—Adult mice (8–16 weeks) of both sexes were used in this study, unless specifically described. *Il23*$^{-/-}$ knockout (KO) mice and *Il23r*$^{-/-}$ (KO) mice were provided by

Genentech under the Material Transfer Agreement (MTA). *Trpv1*$^{-/-}$ mice (JAX 003770), *Trpa1*$^{-/-}$ mice (JAX 006401), nude mice (JAX 001303), *Rag1*$^{-/-}$ mice (JAX 002216) and wildtype (WT) mice (C57BL/6J, JAX 000664) were purchased from the Jackson Laboratory (JAX). *Advillin*^{Cre}*/GCaMP6* mice were generated by crossing *GCaMP6f* mice (JAX 024339) with Advillin-Cre mice (a gift from Fan Wang's lab, Duke University). *Trpv1*^{Cre}*/ERα*$^{fl/fl}$ mice were generated by crossing *Erα*$^{fl/fl}$ mice (JAX 032173) with *Trpv1*-Cre mice (JAX 017769), which were purchased from the Jackson Laboratory. CD1 mice (Charles River Laboratories) were also used for behavioral tests. Animals were randomly assigned to each group. All animals were maintained at the Duke University Animal Facility. Number of animals used in each experiment was described in Table S3. All animal experiments were approved by the Institutional Animal Care and Use Committees of Duke University.

Mouse models of pathological pain—To establish CIPN models, the multiple paclitaxel (PTX) injection model (4 x, 2 mg/kg, I.P., given on day 0, 2, 4, and 6) and the single PTX injection model (6 mg/kg, I.P.) were used in this study. Neuropathic pain was also induced by chronic constriction injury (CCI). Briefly, the left sciatic nerve was exposed at mid-thigh level under isoflurane anesthesia, and three loose silk ligatures (6–0 suture) approximately 1 mm apart were made around the sciatic nerve and the incision was closed with non-absorbable silk suture (5–0) (Luo et al., 2018). To produce diabetic neuropathic pain, mice were given a single intraperitoneal injection of STZ (75 mg/kg), as previously reported (Xu et al., 2015). Acute inflammatory pain was induced by a single intraplantar injection of formalin (5%, 20 μl, Sigma) as previously reported (Luo et al., 2019b).

Peritoneal macrophage culture—Peritoneal macrophages were collected from animals by peritoneal lavage with 10 ml warm PBS containing 1mM of EDTA, as previously reported (Bang et al., 2018). Cells were incubated in DMEM supplemented with 10% FBS at 37 °C for 2 h in a petri dish and washed with PBS to eliminate non-adherent cells. Adherent cells were used in subsequent experiments as peritoneal macrophages following 1 day of culture.

Mouse DRG cultures—DRGs were collected from young mice (4–6 weeks) of both sexes for primary cultures. These cultures were maintained for 16–40 hours for calcium imaging and electrophysiological studies.

NHP and Human DRGs—Non-diseased human DRGs were obtained from donors through National Disease Research Interchange (NDRI) with permission of exemption from the Duke University Institutional Review Board (IRB). Postmortem L3–L5 DRGs were dissected from 4 donors: 18-year-old male, 54-year-old male, 42-year-old female, and 39-year-old female. NHP DRGs were obtained from rhesus macaques (*Macaca mulatta*) in Wake Forest School of Medicine. Lumbar L2-L5 DRGs were collected from three health monkeys: 13-year old female, 10-year old female, and 19-year old male.

METHODS DETAILS

Drug administration in mice—For intraplantar (I.PL.) injection mice were briefly anesthetized with isoflurane (2%) and I.PL. injection was performed on the plantar surface of a hindpaw (10 μl) using a 29G needle to deliver drugs (10 μl) or cells (1×10^5 in 10 μl PBS). For intrathecal injection, mice were briefly anesthetized with isoflurane (2%) and a spinal cord puncture was performed between the L5 and L6 levels to deliver drug (10 μl) using a 29G needle (Luo et al., 2018). For subcutaneous injection, mice were briefly anesthetized with isoflurane (2%) and a subcutaneous injection was performed into the loose skin over the neck to deliver drug (100 μl) using a 29G needle.

Ovariectomy (OVX) and orchidectomy (ORX)—Anaesthetized animals were placed on the operating table with its back exposed. For ovariectomy, a single midline dorsal incision (0.5 cm) was made to penetrate the skin. Subcutaneous connective tissue was gently freed from the underlying muscle on each side using blunt forceps. A small incision (less than 1 cm) was made on each side to gain entry to the peritoneal cavity. Ovary under the thin muscle layer was located and exposed using blunt forceps. Ovary was removed after the oviduct being ligated and severed, and the muscle layer and skin incision were closed by suture. For orchidectomy, a single incision was made on the ventral side of the scrotum. The cremaster muscles were cut, and the testicular fat pad was exposed. A single ligature was made around the blood vessels to prevent bleeding following removal of testis. The skin incision was closed by suture.

Behavioral tests—Behavioral experiments were performed blindly with standard techniques that allow animals to escape from noxious stimuli. For von Frey testing, animals were habituated in boxes on an elevated metal mesh floor under stable room temperature and humidity at least 2 days before the experiments. A series of von Frey fibers with logarithmically increasing stiffness (0.02–2.56 gram, Stoelting) was applied to the plantar surface of the hind-paw, and paw withdrawal threshold (PWT) was calculated using the up-down method (Luo et al., 2018). Thermal hyperalgesia was measured by Hargreaves test using a Hargreaves radiant heat apparatus (IITC Life Science) with a measurement cutoff of 20 seconds to prevent overheating-induced tissue damage. To assess cold allodynia, acetone (20 μl each) was gently applied to the hindpaw bottom using a pipette and the responses to acetone were scored: 0, no response; 1, quick withdrawal, paw stamping or flicking; 2, prolonged withdrawal or repeated flicking of the paw; 3, repeated paw flicking and licking. IL-23-induced ongoing spontaneous pain was examined by conditioned place aversion (CPA) testing (also called place escape avoidance paradigm (LaBuda and Fuchs, 2000)) using a customized two-chamber apparatus positioned on an elevated mesh floor. Mice were allowed to freely explore two chambers for 10 min (pre-stimulation) before the treatment. One hour after receiving I.PL. treatment of IL-23 (100 ng) or the vehicle, each mouse was restricted to one chamber and poked by a 0.04 g von Frey filament for 10 min (stimulation). Each mouse was then allowed to resume moving freely between chambers for 10 min (post-stimulation). Real-time automated video tracking was used to measure movement patterns using ANY-MAZE software.

Flow Cytometry—DRGs were obtained from mice and placed in collagenase A (1 mg/ml, Roche) / dispase II (2.4 U/ml, Roche) in HBSS. DRG tissues were incubated at 37°C with continuous shaking at 100 rpm for 60 min. The cells were dissociated by pipette, washed with HBSS and 0.5% BSA, and filtered through a 70-μm mesh cell strainer. These cells were then treated with 1xRBC lysis buffer (Biolegend) to reduce red blood cell contamination. Dissociated DRGs and peritoneal cells were counted with 2×10^6 cells per sample and fixed by 4% paraformaldehyde (PFA). The cells were blocked and permeabilized by Fc receptor staining buffer [1 μg/ml anti-mouse-CD16/CD32 (101302, Biolegend), 2.4 G2, 2% FBS, 5% NRS, 2% NMS, 0.1% Triton X-100 in HBSS (BD bioscience)] and then stained with a corresponding standard panel of antibodies (see Key resource table) overnight at 4°C. After staining, cells were washed in PBS with EDTA. Flow cytometry events were acquired in a BD FACS Canto II flow cytometer using BD FACS Diva 8 software (BD Bioscience). Gating strategies of flow cytometry are depicted in Table S2. Data were analyzed by Cytobank Software and Flowjo 10.4 (Bang et al., 2018).

ELISA—ELISA kits for mouse IL-23 (433707, Biolegend) and mouse IL-17A/F (DY5390, R&D systems) were used in this study. ELISA tests were performed using DRG tissue lysates, serum samples, and cell culture medium. The DRG tissues were homogenized in a lysis buffer containing protease and phosphatase inhibitors (RIPA buffer, sigma). Blood samples were obtained from heart and allowed to clot for 30 min at 37 °C. After being centrifuged at 2,000 g for 10 min, the supernatants (serum) were collected from the blood samples. The cell culture medium was collected at a volume of 200 μl per sample after application of 1 μg/ml paclitaxel in 1×10^5 seeding cells. For each ELISA assay, 50 μl of lysed DRG proteins, culture medium or serum were used. ELISA tests were conducted according to the manufacturer's instructions. The standard curve was included in each experiment.

Ca^{2+} imaging in cultured mouse DRG neurons—DRGs were collected from young mice (5–8 weeks) of both sexes and incubated with collagenase (1.25 mg/mL, Roche) / dispase-II (2.4 units/mL, Roche) at 37°C for 90 minutes. Cells were plated on glass coverslips precoated with poly-d-lysine and grown in a neurobasal defined medium (with 2% B27 supplement, Invitrogen) with 5% FBS and 5% CO_2 at 37°C for 24 hours before experiment. Ca^{2+} imaging was conducted in DRG neurons from *Advillin-GCaMP6* mice. The calcium imaging buffer included (in mM): 140 NaCl, 5 KCl, 2 $CaCl_2$, 1 $MgCl_2$, 10 HEPES, 10 glucose, adjusted to pH 7.25 with NaOH. Ca^{2+} signals were captured using green emitted light in a 3-second interval. Calcium signal changes were presented as $\Delta F/F_0 = (F_t - F_0)/F_0$, meaning ratio of fluorescence change (F_t - F_0) to basal value (F_0). F_0 represents average fluorescence intensity in the baseline period. F_t represents the fluorescence intensity at each indicated time point (Wang et al., 2020a). To show overall Ca^{2+} signal, we combined all neurons from different experiments together. To quantify percentage of neurons with positive Ca^{2+} response, we included $n \geq 4$ cultures from ≥ 3 mice per group, with exception in Figures S8D–8E due to the limitation of male cKO mice.

Preparation of mouse DRG neurons and whole-cell patch clamp recordings—Neurons were dissociated, plated, and cultured using the same protocol for Ca^{2+} imaging.

Whole-cell voltage-clamp recordings in small-sized DRG neurons (< 25 μm in mice) were conducted at room temperature. Signals were acquired using an Axopatch 200B amplifier. The action potentials were evoked by current injection steps from 0–130 pA with an increment of 10 pA in 600 ms. The data were stored and analyzed with a PC using pCLAMP 10.6 software. Patch pipettes with a pipette solution contained (in mM): 126 potassium gluconate, 10 NaCl, 1 $MgCl_2$, 10 EGTA, 2 Na-ATP, and 0.1 Mg-GTP, adjusted to pH 7.3 with KOH. The external solution included (in mM): 140 NaCl, 5 KCl, 2 $CaCl_2$, 1 $MgCl_2$, 10 HEPES, 10 glucose, adjusted to pH 7.4 with NaOH. In all cases, n refers to the number of the neurons studied from different animals. All drugs were bath applied by gravity perfusion via a three-way stopcock without any change in the perfusion rate (Wang et al., 2020b).

Preparation of NHP DRG neurons and whole-cell patch clamp recordings— Lumbar DRGs were isolated from disease-free monkeys and delivered on ice within 4 h of death. Neurons were dissociated, plated, and cultured as described for mouse DRG neurons. Twenty-four hours after plating, whole-cell patch clamp recordings were performed on small-diameter DRG neurons (<50 μm) at room temperature following the protocol as described for mouse and NHP DRG neurons (Donnelly et al., 2021). The action potentials were evoked by current injection steps from 0–650 pA with an increment of 50 pA in 1,500 ms.

Primary culture and whole cell patch clamp recordings from human DRGs— Non-diseased hDRGs were obtained from three donors through NDRI with permission of exemption from Duke IRB, as previously reported (Wang et al., 2020b; Xu et al., 2015). Postmortem lumbar hDRGs were delivered in ice-cold culture medium within 48–72 h of death. Upon delivery, hDRGs were rapidly dissected from nerve roots and minced in a calcium-free HBSS. hDRGs were digested at 37 °C in a humidified 5% CO2 incubator with a collagenase type II (Worthington, 12 mg/ml final concentration) and dispase II (Roche, 20 mg/ml) solution in HBSS for 120 min. hDRGs were mechanically dissociated using fire-polished pipettes and centrifuged (500g for 5 min). Cells were resuspended, plated on 0.5 mg/ml poly-d-lysine-coated glass coverslips, and grown in culture medium identical to mouse and monkey DRGs. Twenty-four hours after plating, whole-cell patch clamp recordings were performed on small-diameter DRG neurons (<55 μm) at room temperature following the protocol as described for mouse DRG neurons. The action potentials were evoked by current injection steps from 0–130 pA with an increment of 10 pA in 600 ms.

***In situ* hybridization (ISH)—**Mice were deeply anaesthetized with isoflurane and transcardially perfused with PBS followed by 4% paraformaldehyde. Lumbar DRGs (L4-L5) were isolated and post-fixed, and incubated in a sucrose gradient (20–30%). Tissues were then embedded in OCT medium (Tissue-Tek) and cryosectioned with 14 μm-thick DRG sections. *In situ* hybridization was performed using the RNAscope system (Advanced Cell Diagnostics) following the manufacturer's instructions (Wang et al., 2020c). Probes against murine *Il17ra* (403741), *Trpv-1* (313331-C2) and *Era* (478201-C3) were applied in this study. All images were acquired with the same settings, 3 sections from each animal were selected, and a total of four animals per sex were included for data analysis. QuPath software was used for the quantification. Total neuron numbers were determined by counting

DAPI$^+$ nuclei in DRG sections, and visualized cells with more than 3 puncta/cell were classified as positive neurons.

Quantitative real-time RT-PCR (qPCR) in human DRGs—DRG tissues were rapidly isolated in RNAse-free conditions. Total mRNAs were extracted using RNeasy Plus Mini kit (74134, Qiagen) and quantified using a NanoDrop spectrophotometer (Thermo Fisher Scientific). cDNA library of total mRNA was made using high-capacity cDNA reverse transcription kit (4368814, Thermo Fisher Scientific). Primer sequences are depicted in Table S2. qPCR was performed on a QuantStudio 3 Real-Time PCR System (Thermo Fisher Scientific) using PowerUp SYBR Green Master Mix (A25741, Thermo Fisher Scientific). All qPCR results were normalized to h*GAPDH* expression.

QUANTIFICATION AND STATISTICAL ANALYSIS

All data were expressed as the mean ± SEM. The sample size for each experiment was indicated in the figure and figure legend. Statistical analyses were completed with Prism 6 (GraphPad) (Jiang et al., 2020). Behavioral tests, flow cytometry, electrophysiology and ELISA data were analyzed by two-way ANOVA, ordinary or repeated measurement (RM), followed by Bonferroni's post-hoc test or by two-tailed Student's t-test (paired or unpaired). In cases when the data appeared to be non-normally distributed, a normality test was performed (Kolmogorov-Smirnov), followed by a non-parametric Mann-Whitney test. $p < 0.05$ was considered as statistically significant. Please also see Table S4 for more details of statistics for all the related experiments.

ADDITIONAL RESOURCES.

None

Supplementary Material

Refer to Web version on PubMed Central for supplementary material.

ACKNOWLEDEGMENTS

We thank Ji lab members for helpful discussion. We thank Dr. Nico Ghilardi from Genentech for providing the *Il23* and *Il23r* knockout mice. This study was supported by Duke University Anesthesiology Research Funds. The NHP study was supported by NIH grant AR069861. Y.C. was supported by NIH grant DE027454. T.B. was supported by NIH grant NS113243.

DECLARATION OF INTERESTS

Dr. Ji is a consultant of Boston Scientific and received research grant from the company. These activities are not related to this study. Other authors declare no completing interests.

References

Askari A, Naghizadeh MM, Homayounfar R, Shahi A, Afsarian MH, Paknahad A, Kennedy D, and Ataollahi MR (2016). Increased Serum Levels of IL-17A and IL-23 Are Associated with Decreased Vitamin D3 and Increased Pain in Osteoarthritis. PLoS One 11, e0164757. [PubMed: 27820818]

Avona A, Burgos-Vega C, Burton MD, Akopian AN, Price TJ, and Dussor G (2019). Dural Calcitonin Gene-Related Peptide Produces Female-Specific Responses in Rodent Migraine Models. J Neurosci 39, 4323–4331. [PubMed: 30962278]

Avraham O, Deng P-Y, Jones S, Kuruvilla R, Semenkovich CF, Klyachko VA, and Cavalli V (2020). Satellite glial cells promote regenerative growth in sensory neurons. Nature Communications 11, 4891.

Bang S, Xie YK, Zhang ZJ, Wang Z, Xu ZZ, and Ji RR (2018). GPR37 regulates macrophage phagocytosis and resolution of inflammatory pain. J Clin Invest 128, 3568–3582. [PubMed: 30010619]

Basbaum AI, Bautista DM, Scherrer G, and Julius D (2009). Cellular and molecular mechanisms of pain. Cell 139, 267–284. [PubMed: 19837031]

Bian C, Wang ZC, Yang JL, Lu N, Zhao ZQ, and Zhang YQ (2014). Up-regulation of interleukin-23 induces persistent allodynia via CX3CL1 and interleukin-18 signaling in the rat spinal cord after tetanic sciatic stimulation. Brain Behav Immun 37, 220–230. [PubMed: 24362237]

Binshtok AM, Bean BP, and Woolf CJ (2007). Inhibition of nociceptors by TRPV1-mediated entry of impermeant sodium channel blockers. Nature 449, 607–610. [PubMed: 17914397]

Caterina MJ, and Julius D (2001). The vanilloid receptor: a molecular gateway to the pain pathway. AnnuRevNeurosci 24, 487–517.

Chamessian A, Matsuda M, Young M, Wang M, Zhang ZJ, Liu D, Tobin B, Xu ZZ, Van de Ven T, and Ji RR (2019). Is Optogenetic Activation of Vglut1-Positive Aβ Low-Threshold Mechanoreceptors Sufficient to Induce Tactile Allodynia in Mice after Nerve Injury? J Neurosci 39, 6202–6215. [PubMed: 31152125]

Chamessian A, Young M, Qadri Y, Berta T, Ji R-R, and Van de Ven T (2018). Transcriptional Profiling of Somatostatin Interneurons in the Spinal Dorsal Horn. Scientific Reports 8, 6809. [PubMed: 29717160]

Chang W, Berta T, Kim YH, Lee S, Lee SY, and Ji RR (2018). Expression and Role of Voltage-Gated Sodium Channels in Human Dorsal Root Ganglion Neurons with Special Focus on Nav1.7, Species Differences, and Regulation by Paclitaxel. Neurosci Bull 34, 4–12. [PubMed: 28424991]

Chen G, Luo X, Qadri MY, Berta T, and Ji RR (2018a). Sex-Dependent Glial Signaling in Pathological Pain: Distinct Roles of Spinal Microglia and Astrocytes. Neurosci Bull 34, 98–108. [PubMed: 28585113]

Chen G, Zhang YQ, Qadri YJ, Serhan CN, and Ji RR (2018b). Microglia in Pain: Detrimental and Protective Roles in Pathogenesis and Resolution of Pain. Neuron 100, 1292–1311. [PubMed: 30571942]

Chen O, Donnelly CR, and Ji RR (2020a). Regulation of pain by neuro-immune interactions between macrophages and nociceptor sensory neurons. Curr Opin Neurobiol 62, 17–25. [PubMed: 31809997]

Chen Y, Moutal A, Navratilova E, Kopruszinski C, Yue X, Ikegami M, Chow M, Kanazawa I, Bellampalli SS, Xie J, et al. (2020b). The prolactin receptor long isoform regulates nociceptor sensitization and opioid-induced hyperalgesia selectively in females. Sci Transl Med 12.

Diogenes A, Patwardhan AM, Jeske NA, Ruparel NB, Goffin V, Akopian AN, and Hargreaves KM (2006). Prolactin modulates TRPV1 in female rat trigeminal sensory neurons. J Neurosci 26, 8126–8136. [PubMed: 16885226]

Donnelly CR, Jiang C, Andriessen AS, Wang K, Wang Z, Ding H, Zhao J, Luo X, Lee MS, Lei YL, et al. (2021). STING controls nociception via type I interferon signalling in sensory neurons. Nature.

Fillingim RB, King CD, Ribeiro-Dasilva MC, Rahim-Williams B, and Riley JL 3rd (2009). Sex, gender, and pain: a review of recent clinical and experimental findings. J Pain 10, 447–485. [PubMed: 19411059]

Frot M, Feine JS, and Bushnell CM (2004). Sex differences in pain perception and anxiety. A psychophysical study with topical capsaicin. Pain 108, 230–236. [PubMed: 15030942]

Fuseini H, Yung JA, Cephus JY, Zhang J, Goleniewska K, Polosukhin VV, Peebles RS Jr., and Newcomb DC (2018). Testosterone Decreases House Dust Mite-Induced Type 2 and IL-17A-Mediated Airway Inflammation. J Immunol 201, 1843–1854. [PubMed: 30127088]

Gaffen SL, Jain R, Garg AV, and Cua DJ (2014). The IL-23-IL-17 immune axis: from mechanisms to therapeutic testing. Nat Rev Immunol 14, 585–600. [PubMed: 25145755]

Hasegawa H, Abbott S, Han BX, Qi Y, and Wang F (2007). Analyzing somatosensory axon projections with the sensory neuron-specific Advillin gene. The Journal of neuroscience : the official journal of the Society for Neuroscience 27, 14404–14414. [PubMed: 18160648]

He Y, Peng S, Wang J, Chen H, Cong X, Chen A, Hu M, Qin M, Wu H, Gao S, et al. (2016). Ailanthone targets p23 to overcome MDV3100 resistance in castration-resistant prostate cancer. Nature communications 7, 13122.

Hill RZ, and Bautista DM (2020). Getting in Touch with Mechanical Pain Mechanisms. Trends in Neurosciences 43, 311–325. [PubMed: 32353335]

Hou Y, Zhu L, Tian H, Sun HX, Wang R, Zhang L, and Zhao Y (2018). IL-23-induced macrophage polarization and its pathological roles in mice with imiquimod-induced psoriasis. Protein Cell 9, 1027–1038. [PubMed: 29508278]

Ji Y, Tang B, and Traub RJ (2011). Spinal estrogen receptor alpha mediates estradiol-induced pronociception in a visceral pain model in the rat. Pain 152, 1182–1191. [PubMed: 21392887]

Jiang C, Wang Z, Donnelly CR, Wang K, Andriessen AS, Tao X, Matsuda M, Zhao J, and Ji RR (2020). PD-1 Regulates GABAergic Neurotransmission and GABA-Mediated Analgesia and Anesthesia. iScience 23, 101570. [PubMed: 33083737]

Kim CF, and Moalem-Taylor G (2011). Interleukin-17 contributes to neuroinflammation and neuropathic pain following peripheral nerve injury in mice. J Pain 12, 370–383. [PubMed: 20889388]

LaBuda CJ, and Fuchs PN (2000). A Behavioral Test Paradigm to Measure the Aversive Quality of Inflammatory and Neuropathic Pain in Rats. Experimental Neurology 163, 490–494. [PubMed: 10833324]

Lee KM, Zhang Z, Achuthan A, Fleetwood AJ, Smith JE, Hamilton JA, and Cook AD (2020). IL-23 in arthritic and inflammatory pain development in mice. Arthritis Res Ther 22, 123. [PubMed: 32471485]

Lehallier B, Gate D, Schaum N, Nanasi T, Lee SE, Yousef H, Moran Losada P, Berdnik D, Keller A, Verghese J, et al. (2019). Undulating changes in human plasma proteome profiles across the lifespan. Nat Med 25, 1843–1850. [PubMed: 31806903]

Liu XJ, Zhang Y, Liu T, Xu ZZ, Park CK, Berta T, Jiang D, and Ji RR (2014). Nociceptive neurons regulate innate and adaptive immunity and neuropathic pain through MyD88 adapter. Cell Res 24, 1374–1377. [PubMed: 25112711]

Lopes DM, Malek N, Edye M, Jager SB, McMurray S, McMahon SB, and Denk F (2017). Sex differences in peripheral not central immune responses to pain-inducing injury. Sci Rep 7, 16460. [PubMed: 29184144]

Luo H, Liu HZ, Zhang WW, Matsuda M, Lv N, Chen G, Xu ZZ, and Zhang YQ (2019a). Interleukin-17 Regulates Neuron-Glial Communications, Synaptic Transmission, and Neuropathic Pain after Chemotherapy. Cell Rep 29, 2384–2397 e2385. [PubMed: 31747607]

Luo X, Fitzsimmons B, Mohan A, Zhang L, Terrando N, Kordasiewicz H, and Ji RR (2018). Intrathecal administration of antisense oligonucleotide against p38alpha but not p38beta MAP kinase isoform reduces neuropathic and postoperative pain and TLR4-induced pain in male mice. Brain Behav Immun 72, 34–44. [PubMed: 29128611]

Luo X, Gu Y, Tao X, Serhan CN, and Ji R-R (2019b). Resolvin D5 Inhibits Neuropathic and Inflammatory Pain in Male But Not Female Mice: Distinct Actions of D-Series Resolvins in Chemotherapy-Induced Peripheral Neuropathy. Frontiers in pharmacology 10, 745–745. [PubMed: 31333464]

Luo X, Huh Y, Bang S, He Q, Zhang L, Matsuda M, and Ji RR (2019c). Macrophage Toll-like Receptor 9 Contributes to Chemotherapy-Induced Neuropathic Pain in Male Mice. J Neurosci 39, 6848–6864. [PubMed: 31270160]

Ma JN, McFarland K, Olsson R, and Burstein ES (2016). Estrogen Receptor Beta Selective Agonists as Agents to Treat Chemotherapeutic-Induced Neuropathic Pain. ACS Chem Neurosci 7, 1180–1187. [PubMed: 27456785]

Maixner W, and Humphrey C (1993). Gender differences in pain and cardiovascular responses to forearm ischemia. Clin J Pain 9, 16–25. [PubMed: 8477135]

Mapplebeck JCS, Dalgarno R, Tu Y, Moriarty O, Beggs S, Kwok CHT, Halievski K, Assi S, Mogil JS, Trang T, et al. (2018). Microglial P2X4R-evoked pain hypersensitivity is sexually dimorphic in rats. Pain 159, 1752–1763. [PubMed: 29927790]

Meng X, Zhang Y, Lao L, Saito R, Li A, Backman CM, Berman BM, Ren K, Wei PK, and Zhang RX (2013). Spinal interleukin-17 promotes thermal hyperalgesia and NMDA NR1 phosphorylation in an inflammatory pain rat model. Pain 154, 294–305. [PubMed: 23246025]

Mogil JS (2020). Qualitative sex differences in pain processing: emerging evidence of a biased literature. Nat Rev Neurosci 21, 353–365. [PubMed: 32440016]

Niehaus JK, Taylor-Blake B, Loo L, Simon JM, and Zylka MJ (2021). Spinal macrophages resolve nociceptive hypersensitivity after peripheral injury. Neuron 109, 1274–1282. [PubMed: 33667343]

Noor S, Sun MS, Vanderwall AG, Havard MA, Sanchez JE, Harris NW, Nysus MV, Norenberg JP, West HT, Wagner CR, et al. (2019). LFA-1 antagonist (BIRT377) similarly reverses peripheral neuropathic pain in male and female mice with underlying sex divergent peripheral immune proinflammatory phenotypes. Neuroimmunol Neuroinflamm 6.

Patapoutian A, Tate S, and Woolf CJ (2009). Transient receptor potential channels: targeting pain at the source. NatRevDrug Discov 8, 55–68.

Patil M, Belugin S, Mecklenburg J, Wangzhou A, Paige C, Barba-Escobedo PA, Boyd JT, Goffin V, Grattan D, Boehm U, et al. (2019). Prolactin Regulates Pain Responses via a Female-Selective Nociceptor-Specific Mechanism. iScience 20, 449–465. [PubMed: 31627131]

Payrits M, Sághy É, Csekő K, Pohóczky K, Bölcskei K, Ernszt D, Barabás K, Szolcsányi J, Ábrahám IM, Helyes Z, et al. (2017). Estradiol Sensitizes the Transient Receptor Potential Vanilloid 1 Receptor in Pain Responses. Endocrinology 158, 3249–3258. [PubMed: 28977586]

Quiniou C, Dominguez-Punaro M, Cloutier F, Erfani A, Ennaciri J, Sivanesan D, Sanchez M, Chognard G, Hou X, Rivera JC, et al. (2014). Specific targeting of the IL-23 receptor, using a novel small peptide noncompetitive antagonist, decreases the inflammatory response. Am J Physiol Regul Integr Comp Physiol 307, R1216–1230. [PubMed: 25354400]

Richter F, Natura G, Ebbinghaus M, von Banchet GS, Hensellek S, König C, Bräuer R, and Schaible HG (2012). Interleukin-17 sensitizes joint nociceptors to mechanical stimuli and contributes to arthritic pain through neuronal interleukin-17 receptors in rodents. Arthritis Rheum 64, 4125–4134. [PubMed: 23192794]

Riol-Blanco L, Ordovas-Montanes J, Perro M, Naval E, Thiriot A, Alvarez D, Paust S, Wood JN, and von Andrian UH (2014). Nociceptive sensory neurons drive interleukin-23-mediated psoriasiform skin inflammation. Nature 510, 157–161. [PubMed: 24759321]

Shih VF, Cox J, Kljavin NM, Dengler HS, Reichelt M, Kumar P, Rangell L, Kolls JK, Diehl L, Ouyang W, et al. (2014). Homeostatic IL-23 receptor signaling limits Th17 response through IL-22-mediated containment of commensal microbiota. Proc Natl Acad Sci U S A 111, 13942–13947. [PubMed: 25201978]

Simone DA, Baumann TK, and LaMotte RH (1989). Dose-dependent pain and mechanical hyperalgesia in humans after intradermal injection of capsaicin. Pain 38, 99–107. [PubMed: 2780068]

Song C, Luo L, Lei Z, Li B, Liang Z, Liu G, Li D, Zhang G, Huang B, and Feng ZH (2008). IL-17-producing alveolar macrophages mediate allergic lung inflammation related to asthma. J Immunol 181, 6117–6124. [PubMed: 18941201]

Sorge RE, Lacroix-Fralish ML, Tuttle AH, Sotocinal SG, Austin JS, Ritchie J, Chanda ML, Graham AC, Topham L, Beggs S, et al. (2011). Spinal cord Toll-like receptor 4 mediates inflammatory and neuropathic hypersensitivity in male but not female mice. J Neurosci 31, 15450–15454. [PubMed: 22031891]

Sorge RE, Mapplebeck JC, Rosen S, Beggs S, Taves S, Alexander JK, Martin LJ, Austin JS, Sotocinal SG, Chen D, et al. (2015). Different immune cells mediate mechanical pain hypersensitivity in male and female mice. Nat Neurosci 18, 1081–1083. [PubMed: 26120961]

Sun R, Hedl M, and Abraham C (2020). IL23 induces IL23R recycling and amplifies innate receptor-induced signalling and cytokines in human macrophages, and the IBD-protective IL23R R381Q variant modulates these outcomes. Gut 69, 264–273. [PubMed: 31097538]

Tavares-Ferreira D, Ray PR, Sankaranarayanan I, Mejia GL, Wangzhou A, Shiers S, Uttarkar R, Megat S, Barragan-Iglesias P, Dussor G, et al. (2020). Sex Differences in Nociceptor Translatomes Contribute to Divergent Prostaglandin Signaling in Male and Female Mice. Biol Psychiatry S0006–3223(20)31952–1.

Taves S, Berta T, Liu D-L, Gan S, Chen G, Kim YH, Van de Ven T, Laufer S, and Ji R-R (2016). Spinal inhibition of p38 MAP kinase reduces inflammatory and neuropathic pain in male but not female mice: Sex-dependent microglial signaling in the spinal cord. Brain, Behavior, and Immunity 55, 70–81.

Tonello R, Xie W, Lee SH, Wang M, Liu X, Strong JA, Zhang JM, and Berta T (2020). Local Sympathectomy Promotes Anti-inflammatory Responses and Relief of Paclitaxel-induced Mechanical and Cold Allodynia in Mice. Anesthesiology 132, 1540–1553. [PubMed: 32404819]

van der Fits L, Mourits S, Voerman JS, Kant M, Boon L, Laman JD, Cornelissen F, Mus AM, Florencia E, Prens EP, et al. (2009). Imiquimod-induced psoriasis-like skin inflammation in mice is mediated via the IL-23/IL-17 axis. J Immunol 182, 5836–5845. [PubMed: 19380832]

Wang K, Gu Y, Liao Y, Bang S, Donnelly CR, Chen O, Tao X, Mirando AJ, Hilton MJ, and Ji R-R (2020a). PD-1 blockade inhibits osteoclast formation and murine bone cancer pain. The Journal of Clinical Investigation 130, 3603–3620. [PubMed: 32484460]

Wang Z, Jiang C, He Q, Matsuda M, Han Q, Wang K, Bang S, Ding H, Ko MC, and Ji RR (2020b). Anti-PD-1 treatment impairs opioid antinociception in rodents and nonhuman primates. Sci Transl Med 12.

Wang Z, Jiang C, Yao H, Chen O, Rahman S, Gu Y, Zhao J, Huh Y, and Ji RR (2020c). Central opioid receptors mediate morphine-induced itch and chronic itch via disinhibition. Brain 144, 665–681.

Warwick CA, Shutov LP, Shepherd AJ, Mohapatra DP, and Usachev YM (2019). Mechanisms underlying mechanical sensitization induced by complement C5a: the roles of macrophages, TRPV1, and calcitonin gene-related peptide receptors. Pain 160, 702–711. [PubMed: 30507785]

Woolf CJ, and Ma Q (2007). Nociceptors--noxious stimulus detectors. Neuron 55, 353–364. [PubMed: 17678850]

Xu ZZ, Kim YH, Bang SS, Zhang Y, Berta T, Wang F, Oh SB, and Ji RR (2015). Inhibition of mechanical allodynia in neuropathic pain by TLR5-mediated A-fiber blockade. Nature Medicine 21, 1326–1331.

Yamagata K, Sugimura M, Yoshida M, Sekine S, Kawano A, Oyamaguchi A, Maegawa H, and Niwa H (2016). Estrogens Exacerbate Nociceptive Pain via Up-Regulation of TRPV1 and ANO1 in Trigeminal Primary Neurons of Female Rats. Endocrinology 157, 4309–4317. [PubMed: 27689413]

Yu X, Liu H, Hamel KA, Morvan MG, Yu S, Leff J, Guan Z, Braz JM, and Basbaum AI (2020). Dorsal root ganglion macrophages contribute to both the initiation and persistence of neuropathic pain. Nat Commun 11, 264. [PubMed: 31937758]

Zhang X, Huang J, and McNaughton PA (2005). NGF rapidly increases membrane expression of TRPV1 heat-gated ion channels. Embo j 24, 4211–4223. [PubMed: 16319926]

Zheng Y, Liu P, Bai L, Trimmer JS, Bean BP, and Ginty DD (2019). Deep Sequencing of Somatosensory Neurons Reveals Molecular Determinants of Intrinsic Physiological Properties.Neuron.

Zhong YQ, Li KC, and Zhang X (2010). Potentiation of excitatory transmission in substantia gelatinosa neurons of rat spinal cord by inhibition of estrogen receptor alpha. Mol Pain 6, 92. [PubMed: 21143988]

Zhu X, Mulcahy LA, Mohammed RA, Lee AH, Franks HA, Kilpatrick L, Yilmazer A, Paish EC, Ellis IO, Patel PM, et al. (2008). IL-17 expression by breast-cancer-associated macrophages: IL-17 promotes invasiveness of breast cancer cell lines. Breast Cancer Res 10, R95. [PubMed: 19014637]

Zychlinsky Scharff A, Rousseau M, Lacerda Mariano L, Canton T, Consiglio CR, Albert ML, Fontes M, Duffy D, and Ingersoll MA (2019). Sex differences in IL-17 contribute to chronicity in male versus female urinary tract infection. JCI Insight 5.

Highlights

- IL-23 is sufficient to induce mechanical pain in female but not male mice
- This mechanical pain requires sex hormone, macrophages, IL-17A release, and TRPV1
- Low dose IL-17A only activates female nociceptors of mouse and NHP
- IL-23/IL-17A-induced mechanical pain requires estrogen receptor α in nociceptors

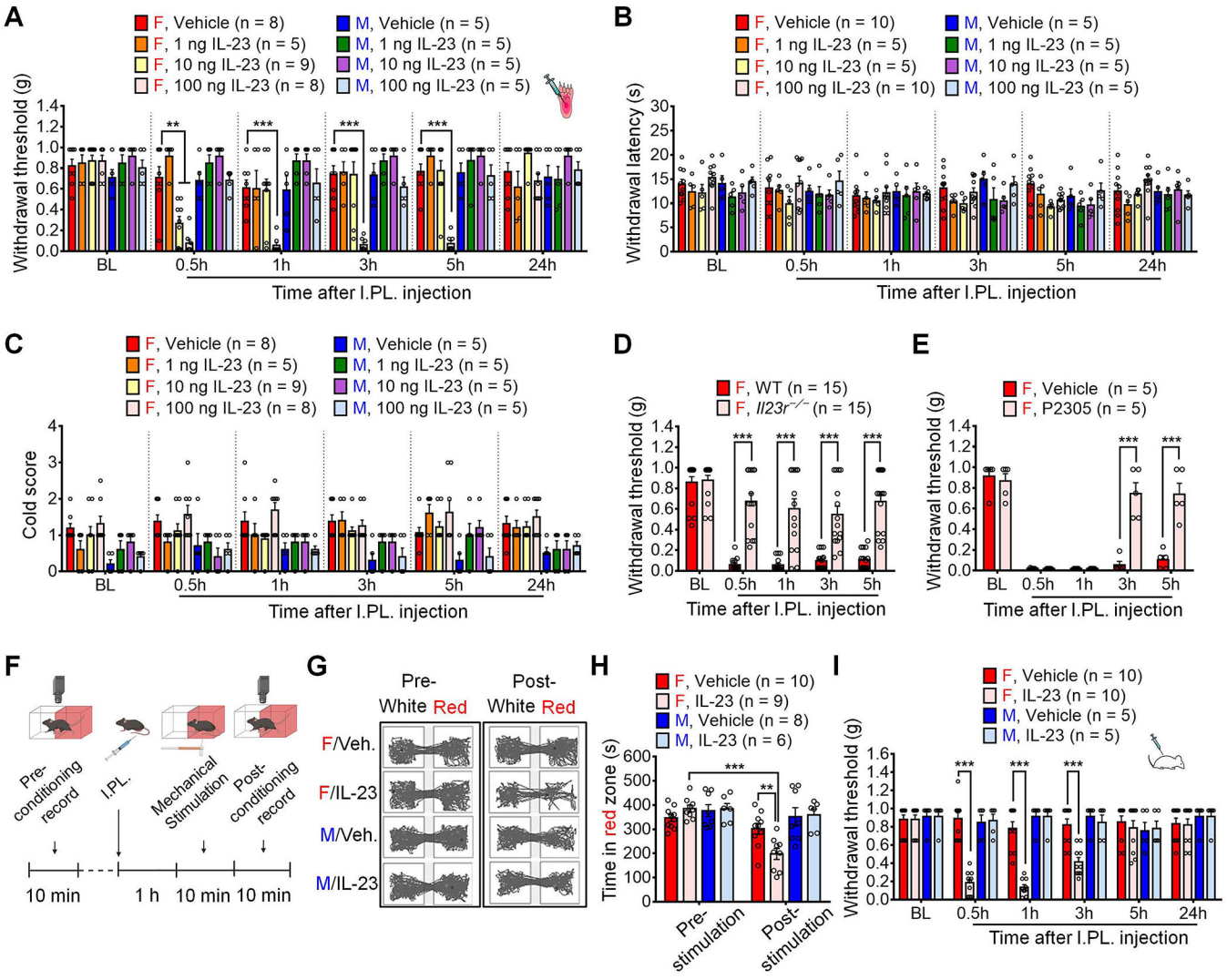

Figure 1. IL-23 induces mechanical pain in female but not male mice.

(A) I.PL. injection of IL-23 at 1, 10 or 100 ng induces dose-dependent mechanical allodynia in female but not male mice compared to the vehicle.

(B-C) I.PL. IL-23 fails to induce thermal hyperalgesia (B, Hargreaves test) or cold allodynia (C, Acetone test) in either sex.

(D-E) Mechanical pain induced by IL-23 (I.PL., 100 ng) in females is abolished in *Il23r*$^{-/-}$ mice (D) and suppressed by IL-23R antagonist P2305 (I.PL., 10 μg, 30 min before IL-23 injection) in WT mice (E).

(F-H) Brief protocol of CPA test (F) and representative traces in two chambers following vehicle and IL-23 (I.PL., 100 ng) treatment (G). (H) CPA test indicates that von Frey stimulation (0.04 g) produces aversive behavior in IL-23-treated female mice (I.PL., 100 ng, 1 h before stimulation) but not males.

(I) Intrathecal IL-23 (I.T., 100 ng) produces mechanical allodynia in female but not male mice.

Data are mean ± SEM. **p < 0.01, ***p < 0.001; Two-Way RM ANOVA with Bonferroni's post hoc test (A-E and H-I). $F_{(35, 252)} = 4.405$ (A); $F_{(35, 210)} = 0.9888$ (B); $F_{(35, 210)} =$

0.9914 (C); $F_{(4,112)} = 11.73$ (D); $F_{(4, 32)} = 20.56$ (E); $F_{(3, 29)} = 8.907$ (H); and $F_{(15, 130)} = 11.19$ (I).

I.PL.: Intraplantar; I.T.: Intrathecal; CPA: Conditioned preference aversion; BL, baseline.

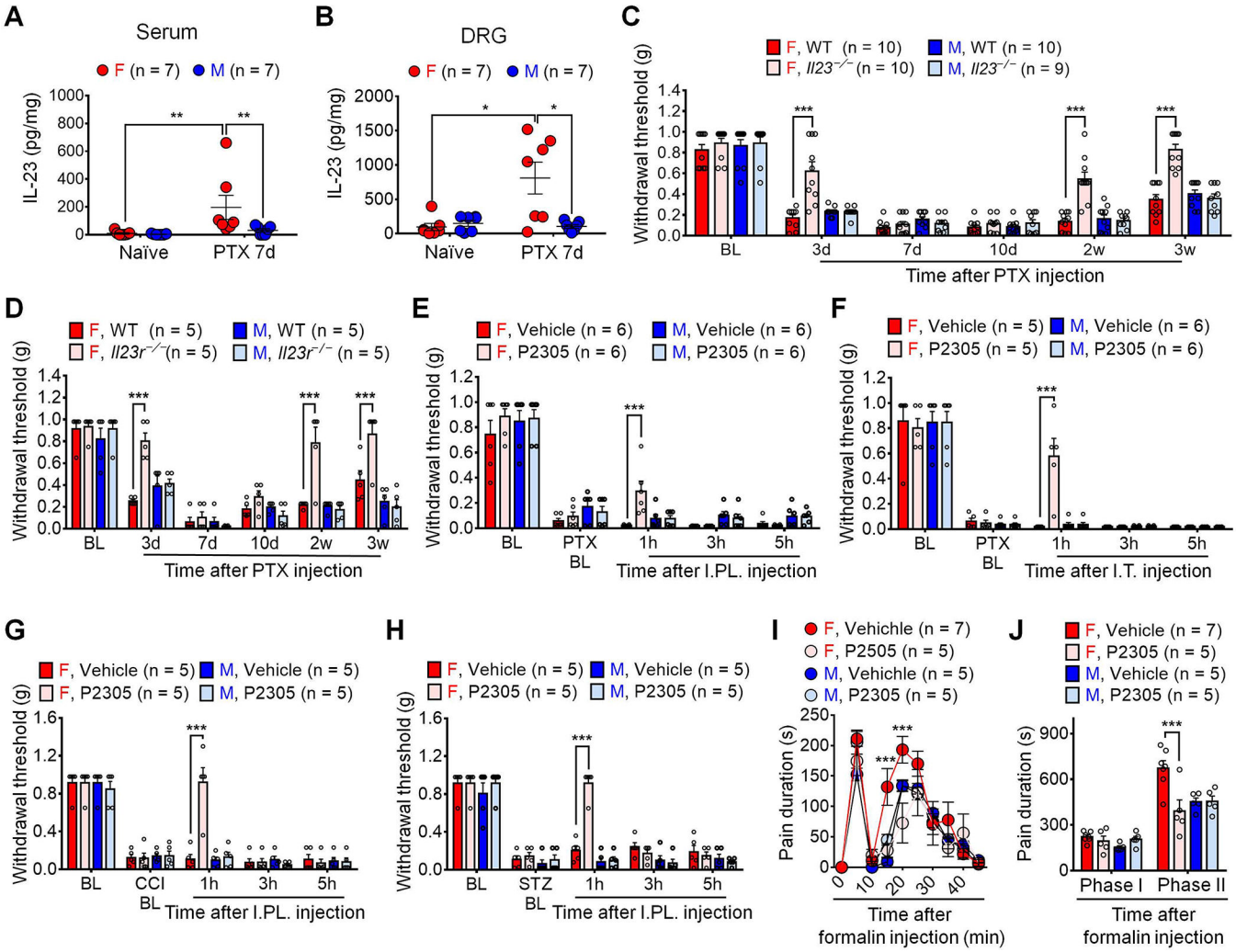

Figure 2. IL-23/IL-23R axis regulates pathological pain in female but not male mice.

(A-B) ELISA showing increased serum (A) and DRG (B) levels of IL-23 in female mice on day 7 after PTX treatment (4 x PTX, 2 mg/kg).

(C-D) PTX-evoked mechanical allodynia is reduced in *Il23*$^{-/-}$ (C) and *Il23r*$^{-/-}$ (D) female mice in CIPN (1 x PTX, 6 mg/kg).

(E-F) P2305 (10 μg), given by I.PL. injection (E) or I.T. injection (F), reduces PTX-induced mechanical allodynia in female but not male mice (4 x PTX, 2 mg/kg).

(G-H) P2305 (I.PL., 10 μg) reduces mechanical allodynia in females in the CCI model (G) and STZ model (H) of neuropathic pain.

(I-J) P2305 (10 μg, I.T., 30 min before I.PL. 5% formalin) reduces formalin-evoked spontaneous pain in females. (I) Time course. (J) Phase I (0–10 min) and Phase II (10–45 min) responses.

Data are mean ± SEM. *p < 0.05, **p < 0.01, ***p < 0.001; Non-parametric Mann-Whitney test (A and B);

Two-Way RM ANOVA with Bonferroni's post hoc test (C-J). $F_{(15, 175)} = 7.090$ (C); $F_{(15, 80)} = 4.781$ (D); $F_{(12, 80)} = 1.746$ (E); $F_{(12, 72)} = 5.353$ (F); $F_{(12, 64)} = 9.924$ (G); $F_{(12, 64)} = 15.03$ (H); $F_{(27, 162)} = 2.359$ (I); $F_{(3, 18)} = 7.333$ (J).

PTX: Paclitaxel; I.T.: Intrathecal; I.PL.: Intraplantar; CIPN: Chemotherapy-induced peripheral neuropathy; CCI: Chronic constrictive injury; STZ: Streptozotocin; BL: Baseline.

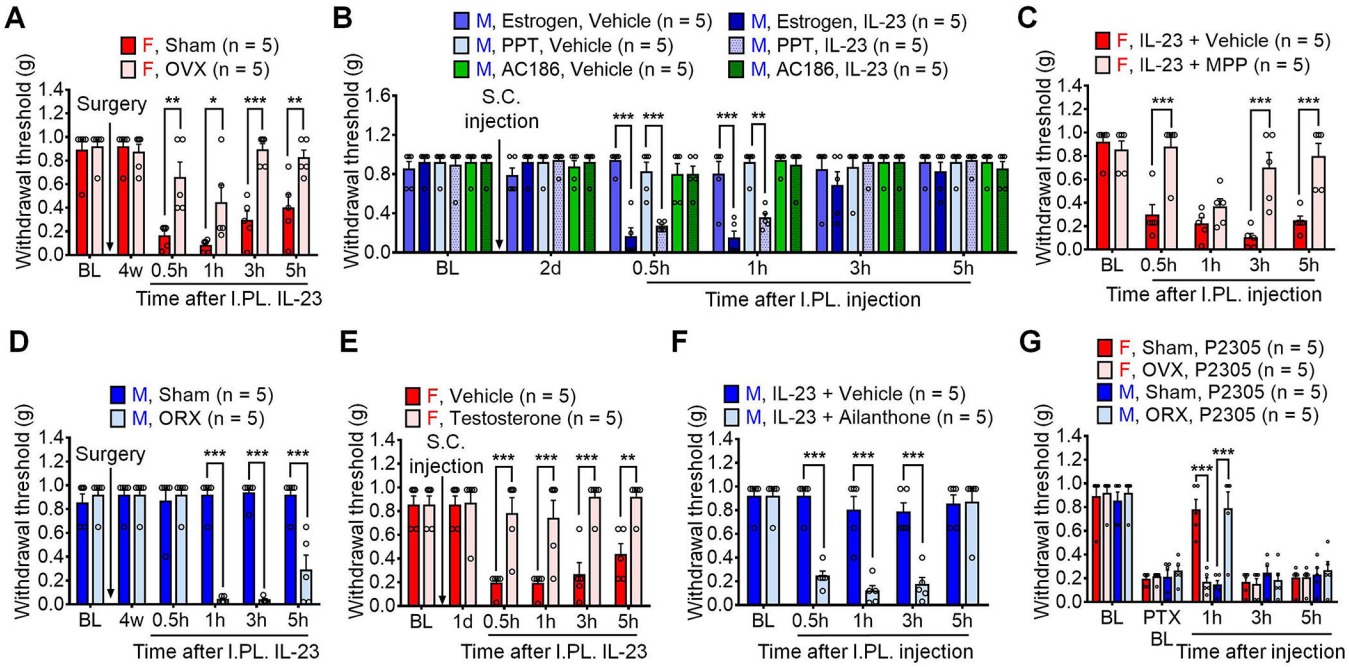

Figure 3. Sex hormones regulate IL-23/IL-23R-mediated pain.

(A) Estrogen deficiency by OVX reduces IL-23-induced pain in female mice.

(B) S.C. pretreatment (2 mg/kg) of estrogen or ERα agonist PPT, but not ERβ agonist AC186, enables IL-23-induced pain (I.PL., 100 ng) in males.

(C) Co-I.PL. injection of ERα receptor antagonist MPP (30 μg) with IL-23 (100 ng) reduces IL-23-induced pain in males.

(D) Androgen deficiency by ORX enables IL-23-induced pain in male mice.

(E) Testosterone treatment (S.C., 2 mg/kg) suppresses IL-23-induced pain (I.PL., 100 ng) in females.

(F) Co-intraplantar injection of androgen receptor antagonist Ailanthone (30 μg) with IL-23 (100 ng) enables IL-23-induced pain in males.

(G) Estrogen deficiency abolishes P2305-produced analgesia (I.PL., 10 μg) in females, whereas androgen deficiency enables P2305-produced analgesia (I.PL., 10 μg) in males in CIPN (7d, 1 x PTX, 6 mg/kg).

Data are mean ± SEM. *p < 0.05, **p < 0.01, ***p < 0.001; Two-way RM ANOVA with Bonferroni's post hoc test; $F_{(5, 40)} = 6.348$ (A); $F_{(25, 120)} = 5.896$ (B); $F_{(4, 32)} = 8.470$ (C); $F_{(5, 40)} = 26.84$ (D); $F_{(5, 40)} = 10.74$ (E); $F_{(4, 40)} = 14.26$ (F); and $F_{(12, 64)} = 6.988$ (G). OVX: Ovariectomy; ORX: Orchiectomy; I.PL.: Intraplantar; S.C.: Subcutaneous; ER: Estrogen receptor; BL: Baseline.

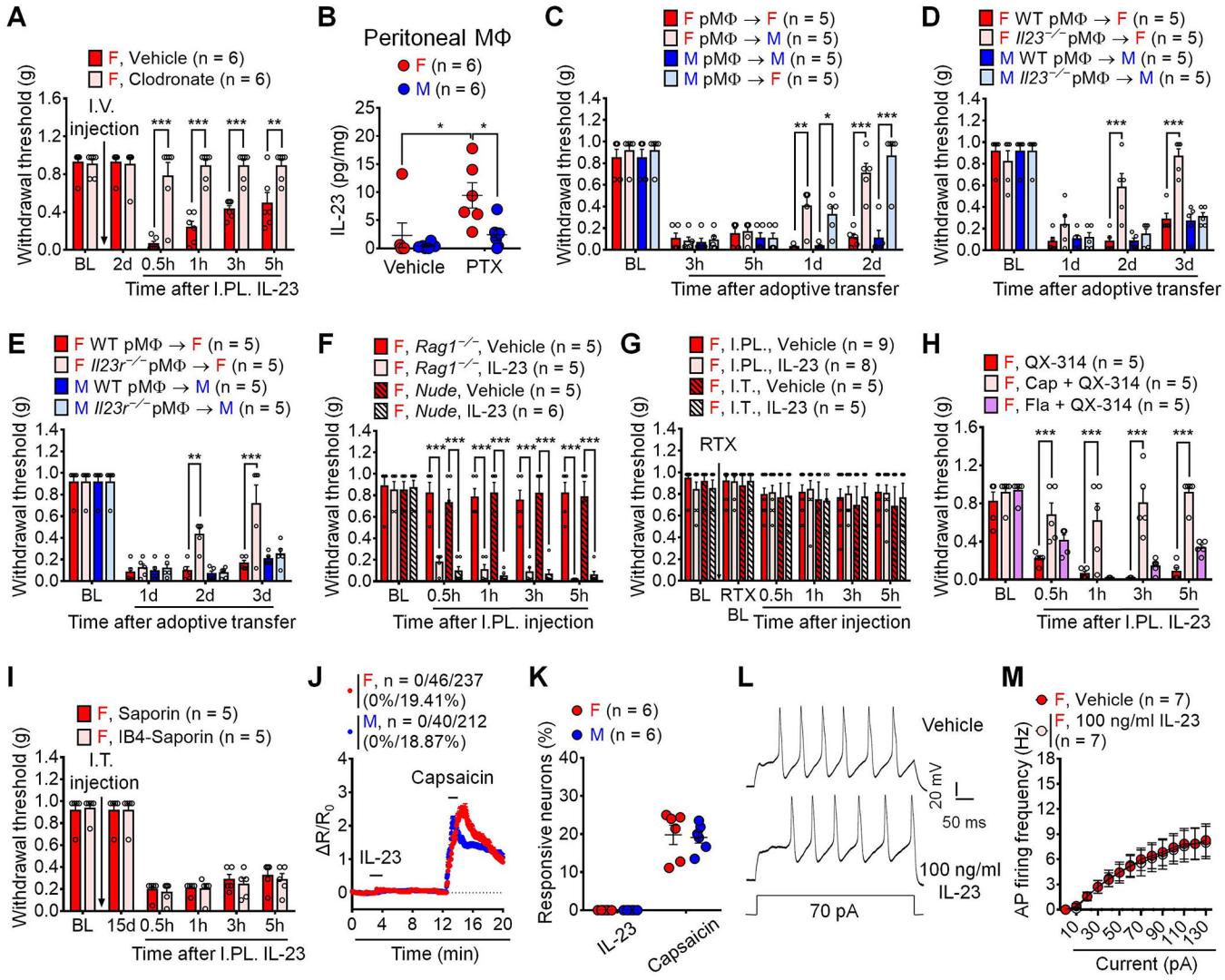

Figure 4. IL-23/IL-23R axis-mediated pain requires macrophages and C-fiber nociceptors.

(A) Clodronate (I.V., 1 mg / 200 μl) abolishes IL-23-induced pain (I.PL., 100 ng) in females.

(B) ELISA showing PTX (1 μg/ml, 16 h) enhanced IL-23 release from female but not male peritoneal macrophages *in vitro*.

(C) PTX-pretreated macrophages (1 μg/ml, 16 h, 10^5 cells) produce more potent and sustained pain in same sex vs. opposite sex recipients.

(D-E) Loss of IL-23 (*Il23*$^{-/-}$, D) or IL-23 receptor (*Il23r*$^{-/-}$, E) attenuates mechanical pain by PTX-pretreated macrophages (1 μg/ml, 16 h, 10^5 cells) in females.

(F) IL-23 (I.PL., 100 ng) induced mechanical allodynia is intact in female mice lacking T cells in *Rag1*$^{-/-}$ mice or nude mice.

(G) RTX-induced C-fiber elimination abolishes mechanical allodynia by IL-23-induced (I.PL. or I.T., 100 ng) in females.

(H) Blockade of TRPV1$^+$ (peptidergic) C-fibers (6 mM QX314 + 5 μg capsaicin) but not TLR5$^+$ Aβ fibers (6 mM QX314 + 0.3 μg flagellin) reduces IL-23-induced mechanical pain in females (I.PL., 100 ng).

(I) Blockade of IB4-binding non-peptidergic C-fibers by IB4-Saporin (I.T. 1.5 μg) fails to affect IL-23-induced pain (I.PL., 100 ng).

(J-K) Effects of IL-23 (100 ng/ml, 2 min) and capsaicin (300 nM, 2 min) on Ca^{2+} influx in dissociated DRG sensory neurons from *Advillin*^{Cre}*/GCamp6f* mice. (J) Combined Ca^{2+} responses from all neurons. Among 237 female neurons, 0 (0%) and 46 (19.41%) show responses to IL-23 and capsaicin, respectively. Among 212 male neurons, 0 (0%) and 40 (18.87%) show responses to IL-23 and capsaicin, respectively. (K) Quantification of % neurons responding to each treatment. n = 6 cultures from 3 mice per sex.

(L-M) IL-23 (100 ng/ml, 2 min) does not potentiate action potentials in dissociated small-sized DRG neurons from females. (L) Traces of action potentials. (M) Firing rate of action potentials.

Data are mean ± SEM. *p < 0.05, **p < 0.01, ***p < 0.001; Two-way RM ANOVA with Bonferroni's post hoc test (A, C-I, M); Two-way ordinary ANOVA with Bonferroni's post hoc test (B); $F_{(5, 50)} = 13.30$ (A); $F_{(1, 20)} = 2.377$ (B); $F_{(12, 64)} = 9.161$ (C); $F_{(9, 48)} = 6.432$ (D); $F_{(9, 48)} = 4.139$ (E); $F_{(12, 68)} = 7.357$ (F); $F_{(15, 115)} = 0.2149$ (G); $F_{(8, 48)} = 5.838$ (H); $F_{(5, 40)} = 0.2094$ (I); $F_{(13, 78)} = 14.48$ (M). Unpaired two-tailed Student's t test, t = 0.2307 (K).

I.V.: intravenous; I.PL.: Intraplantar; I.T.: Intrathecal; PTX: Paclitaxel; RTX: Resiniferatoxin; MΦ: Macrophage; CAP: Capsaicin; BL: Baseline.

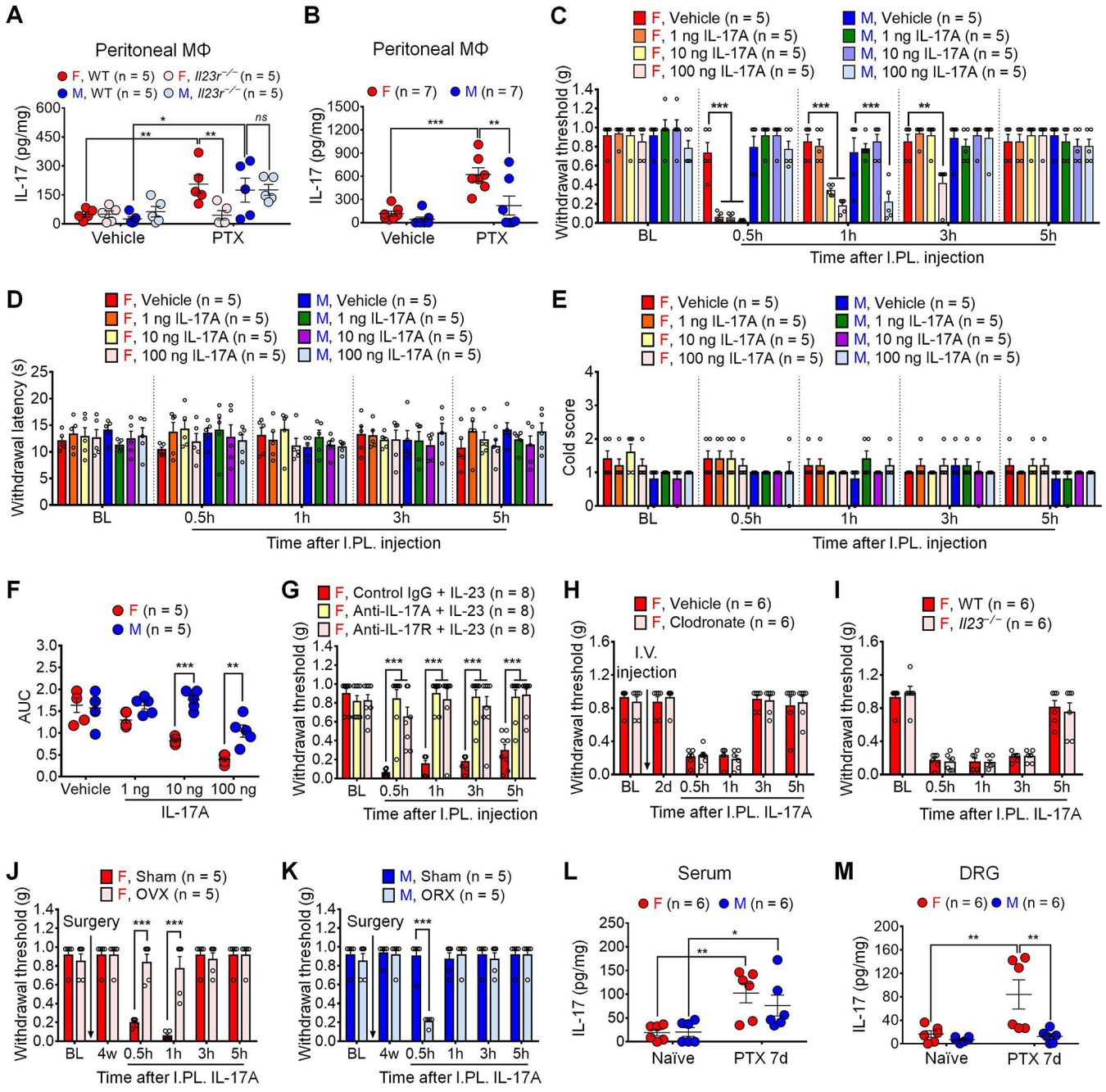

Figure 5. Low doses of IL-17A induce female-dominant mechanical pain.

(A) PTX (1 μg/ml, 16h) promotes IL-17 release from both female and male peritoneal macrophages *in vitro*, which is abolished by *Il23r*$^{-/-}$ only in females.

(B) IL-23 incubation (100 ng/ml, 16h) induces greater IL-17 release from female peritoneal macrophages than male counterparts *in vitro.*

(C) I.PL. IL-17A induces mechanical pain in females at 1–100 ng and males only at 100 ng.

(D-E) I.PL. IL-17A at 1–100 ng fails to induce heat hyperalgesia (D) or cold hypersensitivity (D) in either sex.

(F) AUC (0.5–3h) of Fig. 5C showing female-dominant mechanical pain by IL-17A (10 and 100 ng).
(G) Co-I.PL. injection of IL-17A neutralizing antibody or IL-17RA neutralizing antibody (2 μg) with IL-23 (100 ng) abolishes IL-23-induced pain in females.
(H) Clodronate (I.V., 1 mg / 200 μl) does not affect IL-17A-induced pain (I.PL., 10 ng) in females.
(I) IL-17A (I.PL., 100 ng) induces mechanical allodynia in female *Il23*$^{-/-}$ mice.
(J) Estrogen deficiency by OVX reduces IL-17A-induced mechanical pain (I.PL., 10 ng) in females.
(K) Androgen deficiency by ORX enables IL-17A-induced pain (I.PL., 10 ng) in males.
(L-M) PTX increases serum IL-17 in both sexes (L) but enhances DRG IL-17 only in females (M) in CIPN (4 x PTX, 2 mg/kg).
Data are mean ± SEM. *p < 0.05, **p < 0.01, ***p < 0.001; Two-way ordinary ANOVA with Bonferroni's post hoc test (A and B; L and M); Two-way RM ANOVA with Bonferroni's post hoc test (C-H); $F_{(3, 32)} = 2.575$ (A); $F_{(1, 24)} = 4.336$ (B); $F_{(28, 128)} = 8.077$ (C); $F_{(28, 128)} = 0.5004$ (D); $F_{(28, 128)} = 0.9792$ (E); $F_{(3, 32)} = 7.285$ (F); $F_{(8, 84)} = 7.870$ (G); $F_{(5, 50)} = 0.2779$ (H); $F_{(4, 40)} = 0.3429$ (I); $F_{(5, 40)} = 13.05$ (J); $F_{(5, 40)} = 10.26$ (K); $F_{(1, 20)} = 0.7352$ (L); $F_{(1, 20)} = 5.715$ (M).
AUC: Area under curve; PTX: Paclitaxel; I.PL.: Intraplantar; OVX: Ovariectomy; ORX: orchiectomy; BL: Baseline.

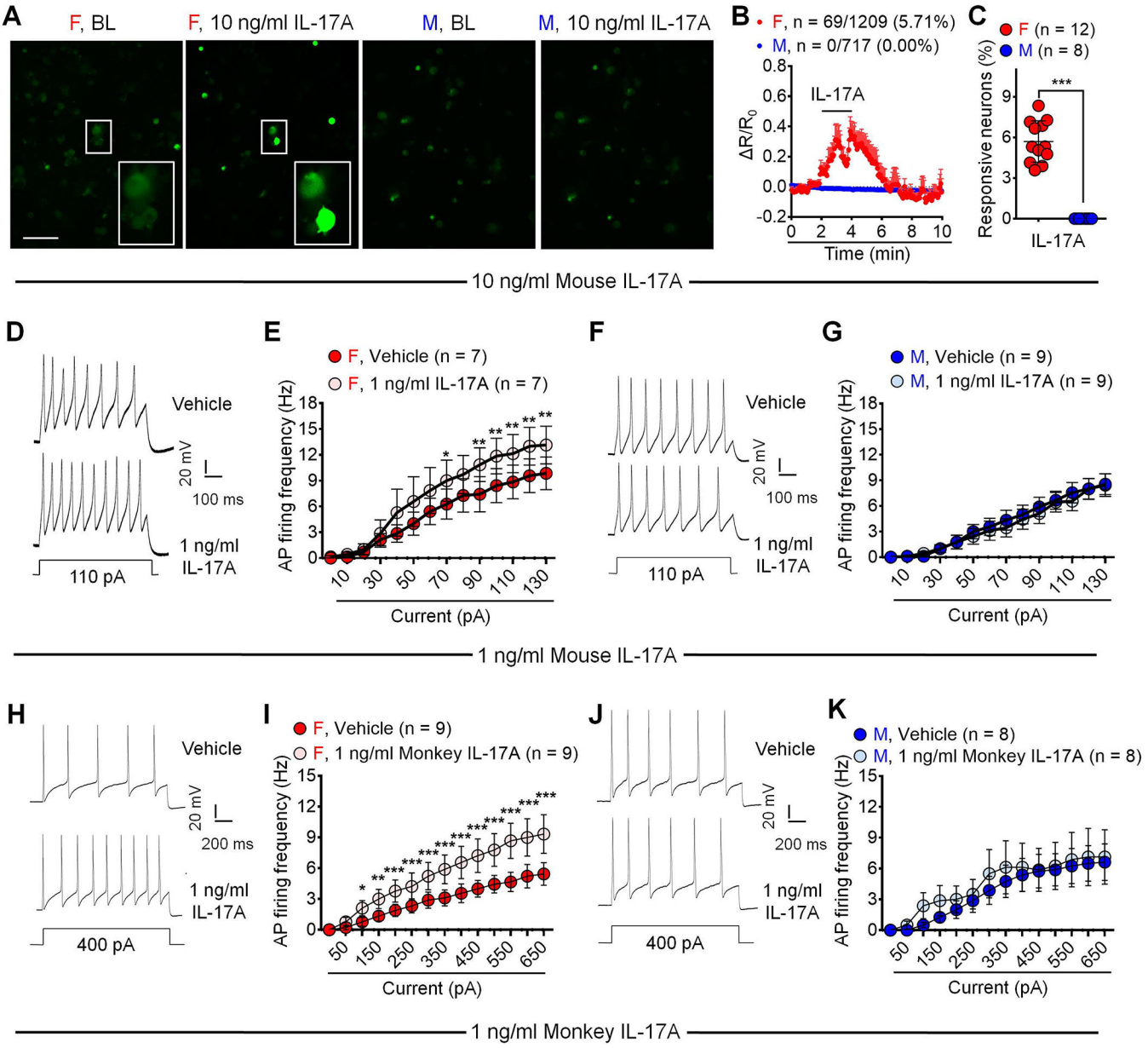

Figure 6. IL-17A activates C-fiber nociceptors in a female-dominant manner.

(A-C) Acute perfusion of IL-17A (10 ng/ml, 2 min) evokes Ca^{2+} influx in DRG sensory neurons cultured from female but not male *Advillin*^{Cre}*/GCamp6f* mice. (A) Representative images. Enlarged images are exhibited in the boxes at the bottom. Scale bar: 100 μm. (B) Combined Ca^{2+} responses of all neurons. 5.71% female neurons (69/1209) and 0% (0/717) male neurons show Ca^{2+} responses. (C) % quantification of responding neurons. n = 8 or 12 cultures from 4 mice of each sex.

(D-G) Bath application of IL-17A (1 ng/ml, 2 min) increases action potential firing in small-sized DRG neurons collected from female but not male mice compared to vehicle. (D, F) Traces of action potentials. (E, G) AP firing rates.

(H-K) AP recordings in NHP DRG neurons. Bath application of monkey IL-17A (1 ng/ml, 2 min) increases AP firing in small-sized DRG neurons collected from female but not male NHP compared to vehicle. (H, J) AP traces. (I, K) AP firing rates.

Data are mean ± SEM. *p < 0.05, **p < 0.01, ***p < 0.001; Unpaired two-tailed student t test, t = 10.44 (C); Two-way RM ANOVA with Bonferroni's post hoc test (E, G, I, K); F values: $F_{(13, 78)} = 23.08$ (E); $F_{(13, 104)} = 26.74$ (G); $F_{(13, 104)} = 25.52$ (I); $F_{(13, 91)} = 9.548$ (K).

AP: Action potential; NHP: Non-human primate. See additional details of statistics in Supplemental information.

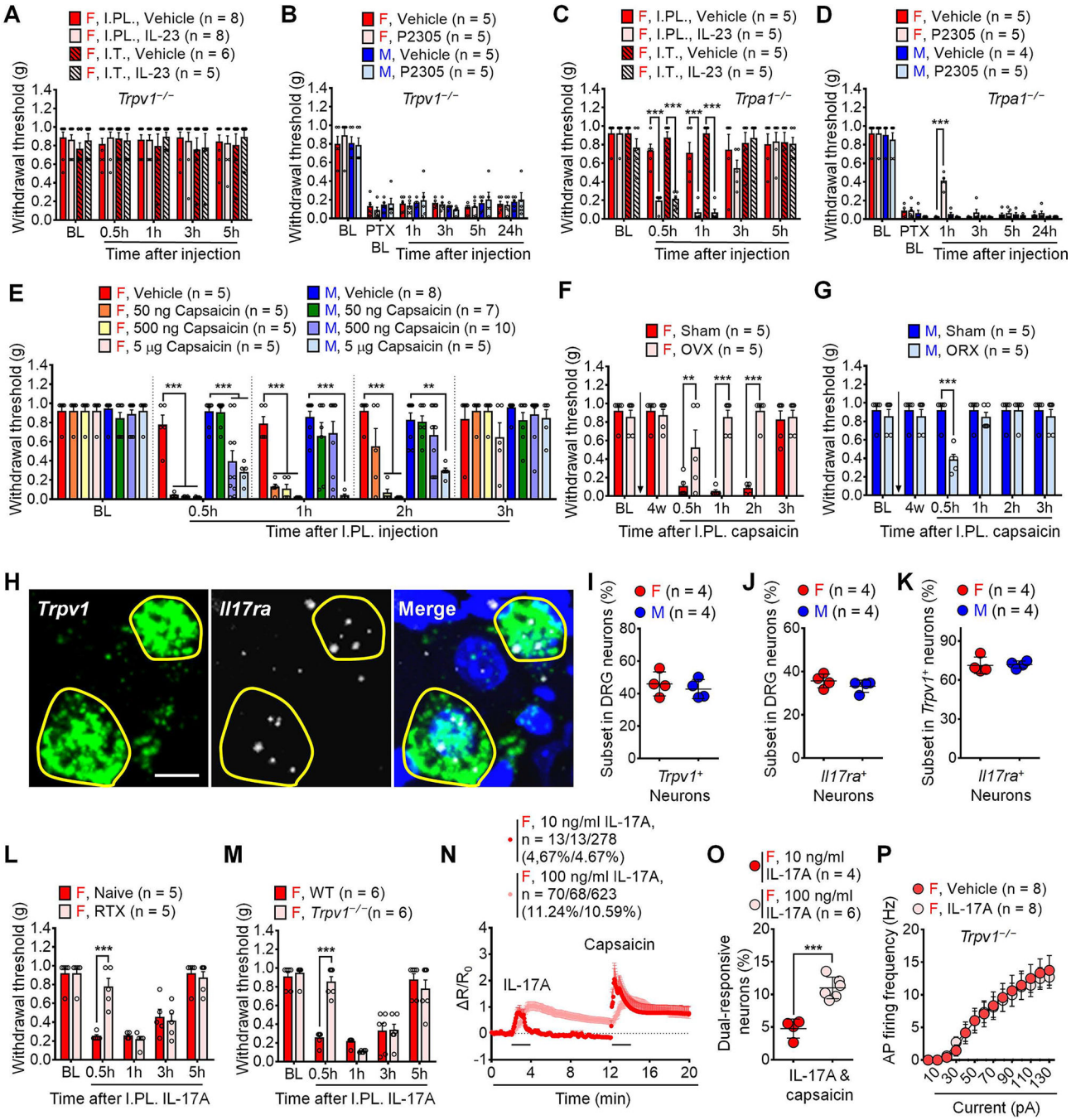

Figure 7. TRPV1 promotes IL-23/IL-17A axis-mediated pain in females.

(A) *Trpv1*$^{-/-}$ abolishes IL-23-induced pain (I.PL. or I.T., 100 ng) in females.

(B) Mechanical pain by PTX (4 × 2 mg/kg) is not affected by IL-23R antagonist P2305 (I.PL., 10 μg) in *Trpv1*$^{-/-}$ mice of both sexes.

(C) IL-23 (I.PL. or I.T., 100 ng) induces comparable mechanical pain in female WT and *Trpa1*$^{-/-}$ mice.

(D) P2305 (I.PL.,10 μg) reduces PTX (4 × 2 mg/kg)-induced mechanical allodynia in female but not male *Trpa1*$^{-/-}$ mice.

(E) I. PL. capsaicin induces mechanical pain in females at 50–5000 ng but males at 500 and 5000 ng.
(F) Estrogen deficiency by OVX reduces capsaicin-induced mechanical pain (I.PL., 500 ng) in females.
(G) Androgen deficiency by ORX promotes capsaicin-induced mechanical pain (I.PL., 500 ng) in males.
(H) *In situ* hybridization (RNAScope) images show co-localization of *Il17ra* and *Trpv1* mRNA in female DRG neurons. Positive neurons are indicated with yellow circles. Blue DAPI staining labels nuclei. Scale bar, 10 μm.
(I-K) Quantification of $Il17ra^{+}$ (I), $Trpv1^{+}$ (J) and $Il17ra^{+}/Trpv1^{+}$ (K) subsets of DRG neurons. n = 4 mice per sex (3 sections per mouse).
(L-M) C-fiber elimination by RTX or $Trpv1^{-/-}$ reduces IL-17A-induced pain (I.PL., 100 ng) in females.
(N-O) Effects of IL-17A (10 and 100 ng/ml, 2 min) and capsaicin (300 nM, 2 min) on Ca^{2+} responses in dissociated DRG sensory neurons from female $Advillin^{Cre}/GCamp6f$ mice. (N) Combined responses of all neurons. 4.67% neurons (13/278) respond to IL-17A (10 ng/ml) and capsaicin, and 11.24% neurons (70/623) respond to IL-17A (100 ng/ml), and 10.91% neurons (68/623) respond to both IL-17A (100 ng/ml) and capsaicin. (O) % quantification of responding neurons. n = 4 or 6 cultures from 3 mice per group.
(P) $Trpv1^{-/-}$ abolishes IL-17A (1 ng/ml, 2 min) potentiation of action potential firing in small-sized DRG neurons from female mice.
Data are mean ± SEM. **p < 0.01, ***p < 0.001; Two-way RM ANOVA with Bonferroni's post hoc test (A-H, L-M, P); $F_{(12, 92)} = 0.2910$ (A); $F_{(15, 80)} = 0.5561$ (B); $F_{(12, 64)} = 6.774$ (C); $F_{(15, 75)} = 5.028$ (D); $F_{(28, 168)} = 7.304$ (E); $F_{(5, 40)} = 13.23$ (F); $F_{(5, 40)} = 4.660$ (G); $F_{(4, 32)} = 8.850$ (L); and $F_{(4, 40)} = 13.90$ (M); $F_{(13, 91)} = 31.63$ (P). Unpaired and two-tailed student t test (I-K, O): t = 0.678 (I); t = 1.160 (J); t = 0.1768 (K); t = 6.119 (O).
I.PL., Intraplantar; I.T., Intrathecal; PTX, Paclitaxel; RTX, Resiniferatoxin; OVX, Ovariectomy; ORX, Orchiectomy; BL, Baseline.

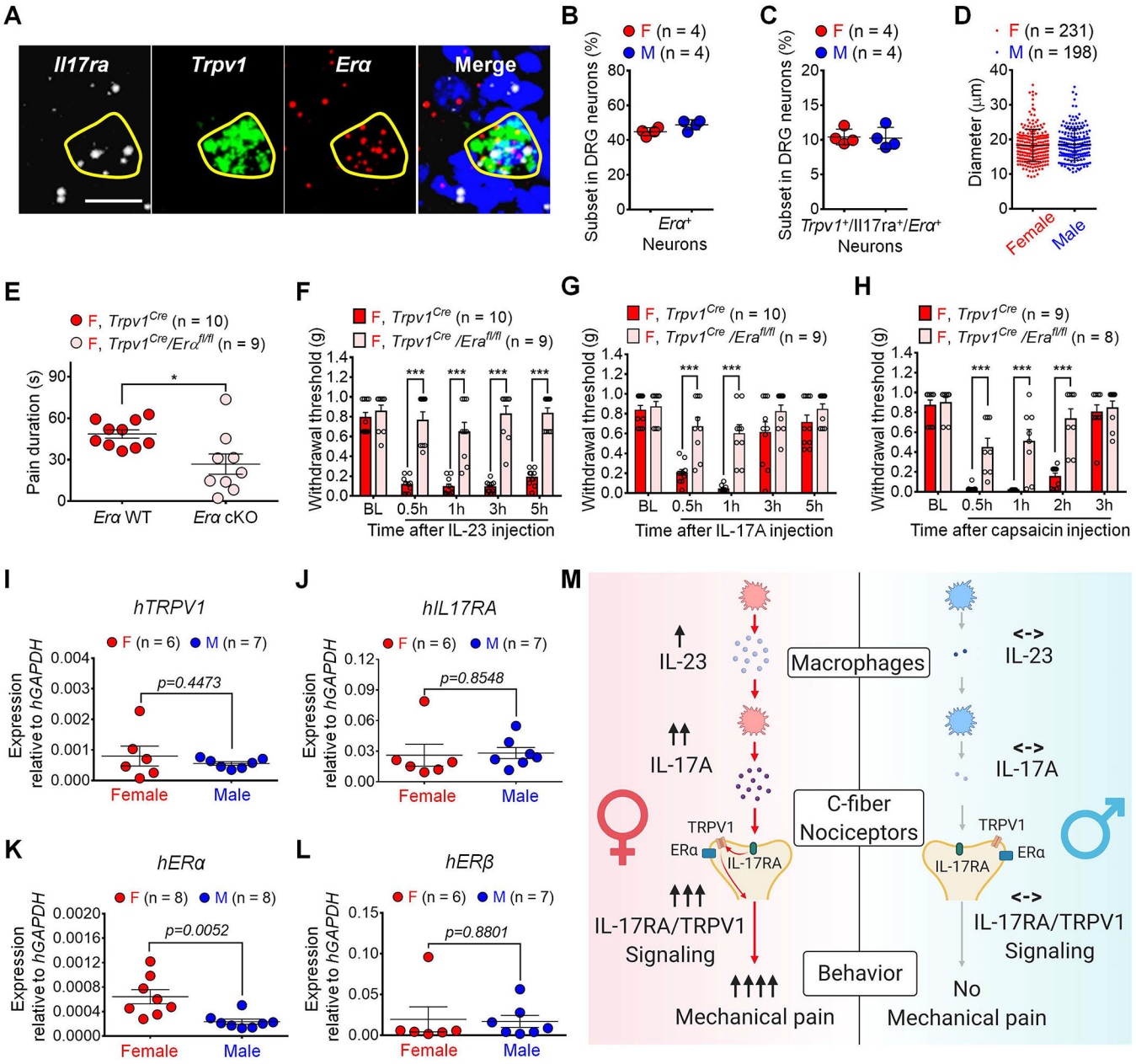

Figure 8. Neuronal estrogen/ERα signaling promotes IL-23/IL-17A-mediated and female-dominant pain.

(A) *In situ* hybridization (RNAScope) showing co-localization of *Il17ra*, *Trpv1* and *Erα* mRNA in DRG neurons (females). Positive neurons are indicated with yellow circles. Scale bar, 10 μm.

(B-C) Quantification of $Erα^+$ neurons (B) and $Il17ra^+/Trpv1^+/Erα^+$ neurons (C) in DRGs. n = 4 mice per sex (3 sections per mouse).

(D) Diameters of $Il17ra^+/Trpv1^+/Erα^+$ neurons in DRGs from both sexes. n = 4 mice per sex (3 sections per mouse).

(E-H) Selective depletion of *Erα* in TRPV1^{+} neurons reduces capsaicin-evoked spontaneous pain (I.PL., 500 ng) in females (E). *Erα* cKO further abolishes mechanical pain, induced by IP.L. IL-23 (100 ng, F), IL-17A (10 ng, G), or capsaicin (500 ng, H) in females.
(I-L) qPCR showing mRNA levels of human *TRPV1* (I), *IL17RA* (J), *ERα* (K) and *ERβ* (L) in DRG tissues from human donors using human *GAPDH* as an internal control. See primer information in Table S2.
(M) Working hypothesis underlying the female-specific modulation of mechanical pain by IL-23/IL-17A/TRPV1 axis. Note that both macrophage and nociceptor signaling contribute to the sex dimorphism.
Data are mean ± SEM. *p < 0.05, ***p < 0.001. Unpaired two-tailed student t test (B-E, I-L): t = 2.142 (B); t = 0.1789 (C); t = 0.6628 (D); t = 2.851 (E); t = 0.7880 (I); t = 0.1874 (J); t = 3.305 (K); t = 0.1544 (L). Two-way ANOVA with Bonferroni's post hoc test (F-H): $F_{(4, 68)} = 15.67$ (F); $F_{(4, 68)} = 5.576$ (G); $F_{(4, 60)} = 9.170$ (H).
I.PL.: Intraplantar; ER: Estrogen receptor; BL: Baseline.

KEY RESOURCES TABLE

REAGENT or RESOURCE	SOURCE	IDENTIFIER
Antibodies		
APC anti-mouse F4/80 antibody	Miltenyl Biotec	Cat# 130-116-525; RRID: AB_2733417
APC/Cy7 anti-mouse/human CD11b antibody	Biolegend	Cat# 101225; RRID: AB_830641
Biotin anti-mouse IL-12/IL-23 p40 antibody	Biolegend	Cat# 505301; RRID: AB_315373
PE anti-mouse IL-23R antibody	Biolegend	Cat# 150903; RRID: AB_2572188
FITC anti-mouse IL-17A antibody	Miltenyl Biotec	Cat# 130-102-262; RRID: AB_2660786
Purified anti-mouse CD16/32 Antibody	Biolegend	Cat# 101302; RRID: AB_312801
LEAF™ purified anti-mouse IL-17A antibody	Biolegend	Cat# 506906; RRID: AB_528927
IL-17R antibody (G-9)	Santa Cruz	Cat# sc-376374; RRID: AB_10991331
Biological Samples		
Monkey DRG tissue	Wake Forest University	NA
Human DRG tissue	National Disease Research interchange (NDRI)	NA
Chemicals, Peptides, and Recombinant Proteins		
Recombinant Mouse IL-23 protein	Biolegend	Cat# 589004
Recombinant Mouse IL-12 protein	Biolegend	Cat# 577002
Recombinant Mouse IL-17A protein	Biolegend	Cat# 576004
Recombinant Cynomolgus monkey IL-17A protein	R&D systems	Cat# 10164-IL-050
Recombinant Human IL-17A protein	Biolegend	Cat# 570504
P2305: Peptide “TEEEEQQLY”	Peptron (Quiniou et al., 2014)	NA
Paclitaxel	Sigma-Aldrich	Cat# T7191
Resiniferatoxin	Sigma-Aldrich	Cat# R8756
AMG9801	Sigma-Aldrich	Cat# A2731
Capsaicin	Sigma-Aldrich	Cat# M2028
QX-314	Sigma-Aldrich	Cat# 552233
Flagellin	InvivoGen	Cat# Tlrl-stfla
IB4-SAP	Advanced targeting systems	Cat# IT-10-25
Saporin	Advanced targeting systems	Cat# SAP-25
eBioscience Streptavidin FITC Conjugate	Invitrogen	Cat# 11-4317-87
PPT	Tocris Bioscience (Ji et al., 2011)	Cat# 1426
MPP	Tocris Bioscienc (Zhong et al., 2010)	Cat# 1991
AC186	Tocris Bioscience (Ma et al., 2016)	Cat# 5030
Ailanthone	Tocris Bioscience (He et al., 2016)	Cat# 6161
17β-Estradiol (Estrogen)	Cayman Chemical	Cat# 10006315
Testosterone	Cayman Chemical	Cat# 15645

REAGENT or RESOURCE	SOURCE	IDENTIFIER
Critical Commercial Assays		
Mouse IL-23 (p19/p40) ELISA kit	Biolegend	433707
Mouse IL-17A/F heterodimer ELISA kit	R&D systems	DY5390
Experimental Models: Organisms/Strains		
Mouse: B6.129X1-*Trpv1*^{tm1Jul} /J (*Trpv1*$^{-/-}$)	The Jackson Laboratory	JAX: 003770
Mouse: B6.129P-*Trpa1*^{tm1Kykw} /J (*Trpa1*$^{-/-}$)	The Jackson Laboratory	JAX: 006401
Mouse: NOD.Cg-*Prkdc*^{scid} / J (nude)	The Jackson Laboratory	JAX: 001303
Mouse: B6.129S7-*Rag1*^{tm1Mom} / J (*Rag1*$^{-/-}$)	The Jackson Laboratory	JAX: 002216
Mouse: B6.129-*Trpv1*$^{tm1(cre)Bbm}$ /J (TRPV1^{CRE})	The Jackson Laboratory	JAX: 017769
Mouse: B6(Cg)-*Esr1*$^{tm4.1Ksk}$ /J (loxERα)	The Jackson Laboratory	JAX: 032173
Mouse: C57BL/6J-Tg(Thy1-GCaMP6f)GP5.11Dkim /J	The Jackson Laboratory	JAX: 024339
Mouse: C57BL/6J (Wildtype)	The Jackson Laboratory	JAX: 000664
Mouse: CD1	Charles River Laboratories	CRL:022
Mouse: *Il23*$^{-/-}$	Genentech (Shih et al., 2014)	NA
Mouse: *Il23r*$^{-/-}$	Genentech (Shih et al., 2014)	NA
Mouse: *Advillin*^{Cre}	Wang lab (Duke) (Hasegawa et al., 2007)	JAX: 032536 |
Oligonucleotides		
Primers for target genes, see Table S2	This paper	NA
RNAscope probe: Mm-*Il17ra*	ACD	Cat# 403741
RNAscope probe: Mm-*Trpv1*-C2	ACD	Cat# 313331-C2
RNAscope probe: Mm-*Esr1*-C3	ACD	Cat# 478201-C3
Software and Algorithms		
ANY-MAZE Software	(Chamessian et al., 2019)	https://www.anymaze.co.uk/
BD FACSDiva™ Software	(Bang et al., 2018)	https://www.bdbiosciences.com/en-us/instruments/research-instruments/research-software/flow-cytometry-acquisition/facsdiva-software
Cytobank Software	(Bang et al., 2018)	https://www.cytobank.org/
Flowjo 10.4	(Chamessian et al., 2018)	https://www.flowjo.com/
QuPath Software	(Wang et al., 2020b)	https://qupath.github.io/
pCLAMP 10.6	(Wang et al., 2020b) Axon	https://mdc.custhelp.com/app/answers/detail/a_id/18779/~/axon%E2%84%A2pclamp%E2%84%A2-10-electrophysiology-data-acquisition-%26-analysis-software-download
Prism 6	(Jiang et al., 2020) GraphPad	https://www.graphpad.com/